

Dynamical properties of small polarons

E.V.L. de Mello[†] and J. Ranninger

Centre de Recherches sur les Très Basses Températures, Laboratoire Associé à l'Université

Joseph Fourier, Centre National de la Recherche Scientifique,

BP 166, 38042, Grenoble Cédex 9, France

(March 30, 2018)

Abstract

On the basis of the two-site polaron problem, which we solve by exact diagonalization, we analyse the spectral properties of polaronic systems in view of discerning localized from itinerant polarons and bound polaron pairs from an ensemble of single polarons. The corresponding experimental techniques for that concern photoemission and inverse photoemission spectroscopy. The evolution of the density of states as a function of concentration of charge carriers and strength of the electron-phonon interaction clearly shows the opening up of a gap between single polaronic and bi-polaronic states, in analogy to the Hubbard problem for strongly correlated electron systems. In studying the details of the intricately linked dynamics of the charge carriers and of the molecular deformations which surround them, we find that in general the dynamical delocalization of the charge carriers helps to strengthen the phase coherence for itinerant polaronic states, except for the crossover regime between adiabatic and anti-adiabatic small polarons. The crossover between these two regimes is triggered by two characteristic time scales: the renormalized electron hopping rate and the renormalized vibrational frequency becoming equal. This crossover regime is then characterized by temporarily alternating self-

localization and delocalization of the charge carriers which is accompanied by phase slips in the charge and molecular deformation oscillations and ultimately leads to a dephasing between these two dynamical components of the polaron problem. We visualize these features by a study of the temporal evolution of the charge redistribution and the change in molecular deformations. The spectral and dynamical properties of polarons discussed here are beyond the applicability of the standard Lang Firsov approach to the polaron problem.

71.38.+i, 63.20.Kr, 72.20.Jv

I. INTRODUCTION

Renewed interest in the physics of small polarons in the last few years has been largely stimulated by the discovery of new materials with exceptional properties such as the High T_c cuprates, the nickelates and the manganites showing giant magneto resistance. It is believed that small polarons play an essential role in these materials. Recently developed experimental techniques such as femto- second optical spectroscopy, EXAFS and pulsed neutron scattering, ionchanneling experiments and high resolution angle resolved photoemission experiments have been employed to study the properties of polaronic systems. In spite of considerable theoretical efforts in the last few years, the underlying physics of the polaron problem has remained largely unresolved.

As concerns the problem of a single polaron in an empty lattice with local coupling of the charge to a set of individual non-interacting local lattice deformations (the Holstein model) it is known that self-trapping of a charge carrier occurs when

i) the gain in localization energy ε_p outweighs the gain in kinetic energy $D/2$, i.e., $g \equiv 2\varepsilon_p/D \geq 1$, D denoting the bare electron bandwidth and

ii) the relative deformation of the lattice which surrounds the charge carrier essentially remains confined to the immediate vicinity of the charge carrier i.e., $2\alpha^2 \equiv \varepsilon_p/\omega_0 \geq 1$, ω_0 denoting the bare local phonon frequency.

A crossover between essentially delocalized quasi-free electrons and self-trapped electrons is known from Quantum Monte Carlo simulations [1] to occur in a regime of parameters characterized by the two conditions i) and ii) for small polaron formation, i.e. for $g \sim 1$ and $\alpha \sim 1$. This crossover regime in α narrows substantially upon going from the anti-adiabatic ($\gamma \equiv t/\omega_0 = 4\alpha^2/(zg) \ll 1$) to the adiabatic ($\gamma \gg 1$) limit with z denoting the coordination number.

The standard theory of small polarons is based on the so called Lang Firsov (LF) transformation usually followed by approximations treating the fully localized polaron state as the starting point of the theory and then introducing the hopping of the electrons by per-

turbative means [2]. There is a widespread (however erroneous) belief that such a scheme is valid in the extreme strong coupling anti-adiabatic limit i.e., $\gamma \ll 1$ and $\alpha \gg 1$. It is not surprising that such theoretical treatment is even less able to describe polarons close to the crossover regime, which represents the physically interesting and realistic situations.

As concerns the problem of the many polaron system the principal difficulty is to take into account the overlap of the lattice deformations surrounding the charge carriers when the density of polarons becomes important. It is expected that, due to destructive interference of such local deformations, the whole concept of polarons breaks down, the lattice changes its structure and as a result the effective electron lattice coupling becomes strongly reduced.

It is the purpose of this present work to obtain some insight into the physics of small polarons for realistic values of the relevant parameters γ and α and in particular close to the crossover regime. Since all known materials containing small polarons consist of highly polarizable small clusters ($Ti^{3+} - Ti^{3+}$ pairs in Ti_4O_7 , $V^{4+} - V^{4+}$ pairs in $Na_xV_2O_5$), sometimes embedded in a metallic background (such as the $O(4)^{2-} - Cu(1)^+ - O(4)^{2-}$ dumbbells in cuprate High T_c superconductors containing chains separating the metallic CuO_2 layers), it is not only instructive from a pedagogical point of view to study small polaron features on the basis of such small units, but such studies may also apply to true physically relevant situations. On the basis of a two-site polaron system (a system consisting of two adjacent molecules between which the electrons can hop) we shall illustrate the highly non-linear physics going on in such a problem. For $\alpha \gg 1$ and $\gamma \ll 1$ (the so called strong coupling anti-adiabatic regime or extreme polaron limit) it will be shown that the dynamics of the fluctuations of the lattice deformations is driven by the charge fluctuations, while for $\alpha \ll 1$ and $\gamma \gg 1$ (the so called weak coupling adiabatic regime) the inverse happens. The crossover regime is characterized by alternating localization and delocalization of the charge carriers as a function of time. In general the amplitude and the frequency of the intrinsic lattice vibrations as well as of the intrinsic electron hopping rate are strongly renormalized. Such effects may turn out to be vital as concerns a mechanism for the damping of polaronic charge carriers; a feature which is inaccessible within the usual LF approach.

The paper is organized in the following way: In section 2 we shall present the model and its basic physics as well as our method of an exact diagonalization study. In section 3 we discuss the dependence of the kinetic energy of the electron on the adiabaticity parameter γ and the coupling strength α and examine the limitations of the LF approach. Section 4 will be devoted to the study of the one particle spectral function in view of distinguishing localized from itinerant polarons and to discern tightly bound polaron pairs (bipolarons) from simple polarons by such methods as photoemission spectroscopy. In section 5 we will study the time evolution of the charge redistribution and of the lattice deformation and discuss the renormalization of the intrinsic lattice vibrational frequency and of the electron hopping integral in the course of the charge transfer process.

II. THE MODEL

The smallest system on which polaronic features can be studied as far as self-trapping, localization-delocalization crossover, frequency renormalization and dephasing of the correlated charge-deformation dynamics is concerned, is the so called two-site polaron system. It consists of two elastically uncoupled adjacent diatomic molecules with atoms having mass M and an intrinsic bare frequency of intra-molecular vibrations ω_0 . Electrons can hop between those two molecules having a bare hopping rate t . In the Holstein model for such a system, the strength of the coupling constant of the density of charge carriers to the intra-molecular deformations is denoted by λ . The model Hamiltonian for such a system is then given by

$$\begin{aligned}
 H = & t \sum_{\sigma} (n_{1\sigma} + n_{2\sigma}) - t \sum_{\sigma} (c_{1\sigma}^{\dagger} c_{2\sigma} + c_{2\sigma}^{\dagger} c_{1\sigma}) - \lambda \sum_{\sigma} (n_{1\sigma} u_1 + n_{2\sigma} u_2) \\
 & + \frac{M}{2} (\dot{u}_1^2 + \dot{u}_2^2) + \frac{M}{2} \omega_0^2 (u_1^2 + u_2^2) + U (n_{1\uparrow} n_{1\downarrow} + n_{2\uparrow} n_{2\downarrow})
 \end{aligned} \tag{1}$$

where $n_{i\sigma} = c_{i\sigma}^{\dagger} c_{i\sigma}$ denotes the density of charge carriers at molecular site i and having spin σ . The intra-molecular deformations are denoted by u_1 and u_2 respectively. We assume a simple form of repulsive intra-molecular Coulomb forces of strength U . The above Hamiltonian Eq.(1) has been extensively studied by a number of authors [3–10] who, by means of exact

diagonalization, have examined various aspects of the polaron problem. Diagonalization of the above Hamiltonian can be rendered more efficient [9] when decomposing it into a term containing the symmetric in-phase lattice vibrations characterized by a wavevector $q = 0$ and antisymmetric out-of-phase vibrations characterized by a wavevector $q = \pi$. The Hamiltonian then can be separated into two independent contributions $H = H_X + H_Y$, given by:

$$H_X = t \sum_{\sigma} (n_{1\sigma} + n_{2\sigma}) - t \sum_{\sigma} (c_{1\sigma}^{\dagger} c_{2\sigma} + c_{2\sigma}^{\dagger} c_{1\sigma}) - \lambda/\sqrt{2} \sum_{\sigma} (n_{1\sigma} - n_{2\sigma}) X + \frac{M}{2} \dot{X}^2 + \frac{M}{2} \omega_0^2 X^2 + U(n_{1\uparrow} n_{1\downarrow} + n_{2\uparrow} n_{2\downarrow}) \quad (2)$$

$$H_Y = \frac{M}{2} \left[\dot{Y} - \frac{\lambda n}{\sqrt{2} M \omega_0^2} \right]^2 + \frac{M}{2} \omega_0^2 \left[Y - \frac{\lambda n}{\sqrt{2} M \omega_0^2} \right]^2 - \frac{\lambda^2 n^2}{4 M \omega_0^2} \quad (3)$$

where

$$X = \frac{u_1 - u_2}{\sqrt{2}} = \frac{a^{\dagger} + a}{\sqrt{2 M \omega_0 / \hbar}} \quad (4)$$

$$Y = \frac{u_1 + u_2}{\sqrt{2}} = \frac{b^{\dagger} + b}{\sqrt{2 M \omega_0 / \hbar}} + \frac{\lambda n}{\sqrt{2} M \omega_0^2} \quad (5)$$

and $a^{(\dagger)}$ and $b^{(\dagger)}$ denote the annihilation (creation) operators of the quantized lattice fluctuations with momentum $q = \pi$ and $q = 0$ respectively. Since in H_Y the phonons couple only to the total charge $n = \sum_{i\sigma} n_{i\sigma}$ of the system, H_Y can be diagonalized exactly since it represents simply a shifted oscillator, corresponding to the two diatomic molecules of our system having their equilibrium positions shifted by equal amounts $u^0 = (\lambda n)/2 M \omega_0^2$. H_X on the contrary contains the full dynamics of the system and has to be diagonalized numerically in terms of a judiciously chosen set of basis states (see ref. [9]) such as

$$|l_X, l_Y\rangle = \sum_{N_X, N_Y}^{\infty} \frac{1}{\sqrt{2}} c_{1,\sigma}^{\dagger} (\alpha_{l_X, N_X}^+ + \alpha_{l_X, N_X}^-) |N_X\rangle \beta_{l_Y, N_Y} |N_Y\rangle + \sum_{N_X, N_Y}^{\infty} \frac{1}{\sqrt{2}} \frac{1}{\sqrt{2}} c_{2,\sigma}^{\dagger} (\alpha_{l_X, N_X}^+ - \alpha_{l_X, N_X}^-) |N_X\rangle \beta_{l_Y, N_Y} |N_Y\rangle \quad (6)$$

for the one-electron two-site problem. $|N_{X,Y}\rangle$ denote the eigenstates of the oscillator part of $H_{X,Y}$ for $\lambda = 0$. The coefficients β_{l_Y, N_Y} are known analytically from the expansion of a

shifted oscillator states in terms of the excited states of the unshifted one. For $l_Y = 0$ we have $\beta_{0,N_Y} = \exp - (\alpha^2/2)\alpha^{N_Y}/\sqrt{N_Y!}$. The coefficients $\alpha_{l_X,l_Y}^{+,-}$ are determined by diagonalizing numerically H_X with in a truncated Hilbertspace of states with up to 100 phonon states, i.e., $0 \leq N_X \leq 100$. The procedure of separating off in the Hamiltonian a part which can be diagonalized exactly represents a substantial reduction in the numerical work of studying polarons not only for our two-site model but in general [11].

Applying the standard LF approach to this problem amounts to using a representation in which the molecules exist in a set of oscillator states: those not containing any electron and being described by the full set of oscillator states labeled by $|\Phi(X)\rangle_m$ and $|\Phi(Y)\rangle_n$, those containing an electron on one of the two sites and being described by shifted oscillator states $|\Phi(X \pm X_0)\rangle_m$ and $|\Phi(Y - Y_0)\rangle_n$, those containing two electrons on one of the two sites and being described by $|\Phi(X \pm 2X_0)\rangle_m$ and $|\Phi(Y - 2Y_0)\rangle_n$ and finally those containing one electron on each site and being described by $|\Phi(X)\rangle_m$ and $|\Phi(Y - 2Y_0)\rangle_n$. The shift in equilibrium positions for the two oscillators are given by $X_0 = Y_0 = \lambda n/\sqrt{2}M\omega_0^2$ and the shifted oscillator states are defined by

$$\begin{aligned} |\Phi(X - X_0)\rangle_m &= \frac{(a^\dagger - \alpha)^m}{\sqrt{m!}} \exp(\alpha[a^\dagger - a]) |\Phi(X)\rangle_0 \\ &= \frac{(a^\dagger - \alpha)^m}{\sqrt{m!}} \sum_l \frac{\alpha^l}{\sqrt{l!}} \exp(-\alpha^2/2) |\Phi(X)\rangle_l \end{aligned} \quad (7)$$

In such a representation the Hamiltonian H_X becomes

$$\begin{aligned} H_X &= t \sum_\sigma (n_{1\sigma} + n_{2\sigma}) - t \sum_\sigma (c_{1\sigma}^\dagger \exp(\alpha[a^\dagger - a]) c_{2\sigma} + H.c.) \\ &\quad - \varepsilon_p n - (2\varepsilon_p - U) \sum_i n_{i\uparrow} n_{i\downarrow} + \hbar\omega_0 (a^\dagger a + \frac{1}{2}) \end{aligned} \quad (8)$$

in which the intricate dynamics of the polaron problem is contained in the modified hopping term (the second term in Eq.(8)) showing a concomitant transfer of charge and deformation. The standard LF approach to this problem is then to consider, to within a first approximation, that the deformation of the molecules follows instantaneously the motion of the electrons, that is to say without any emission or absorption of phonons during the process

which transfers an electron from one site to the other. For our two-site polaron model this implies states of the form

$$|LF\rangle_{mn}^{\pm} = \frac{1}{\sqrt{2}} \left(c_{1\sigma}^{\dagger} |\Phi(X - X_0)\rangle_m \pm c_{2\sigma}^{\dagger} |\Phi(X + X_0)\rangle_m \right) |\Phi(Y - Y_0)\rangle_n \quad (9)$$

which amounts to disentangle the correlated hopping term in the form

$$\begin{aligned} c_{1\sigma}^{\dagger} \exp(\alpha[a^{\dagger} - a]) c_{2\sigma} &\Rightarrow \\ c_{1\sigma}^{\dagger} c_{2\sigma} \langle \exp(\alpha[a^{\dagger} - a]) \rangle_{H_{ph}} &= t_{LF}^* c_{1\sigma}^{\dagger} c_{2\sigma} \end{aligned} \quad (10)$$

This way one obtains an effective Hamiltonian to start with and subsequently treats the remainder of the full Hamiltonian in a perturbative way - corresponding to an expansion in terms of $1/\lambda$ [12]. The average in Eq.(10) is taken over the free phonon Hamiltonian H_{ph} , given by the last term in Eq.(8) and which leads to $t_{LF}^* = t \exp(-2\alpha^2)$. For a many polaron problem, polaronic states may become unstable with respect to bi-polaron formation provided the Coulomb repulsion U is overcome. This then leads to states of the form $c_{i\uparrow}^{\dagger} c_{i\downarrow}^{\dagger} |\Phi(X \pm 2X_0)\rangle_m |\Phi(Y \pm 2Y_0)\rangle_n$. Upon eliminating single polaron states in the Hamiltonian, Eq(1) one derives [13] an effective Hamiltonian describing bi-polaronic hopping with a hopping integral $t_{LF}^{**} = (t^2/(2\varepsilon_p)) \exp(-4\alpha^2)$ for $U = 0$.

III. INTERSITE CHARGE TRANSFER AND MULTIPLE HOPPING PROCESSES

It has remained a question of dispute as how good the LF approach is and whether in the extreme polaronic limit the LF approximation, i.e. the substitution described by Eq.(10), becomes exact. If this is not the case, then a perturbation theory in terms of $1/\lambda$ can not be applied to the polaron problem. It has for a long time been taken as granted that the problem of a single polaron in an infinite lattice of finite dimension is described by polaron band states having a k dependent dispersion identical to that of the bare electron but with a reduced bandwidth $2zt^*$, where z denotes the coordination number. There are

now indications from exact diagonalization studies of finite clusters [14] that this is not correct and that the k dependence of the dispersion differs significantly from that of the bare electrons. From exact diagonalisation studies [9,10] of the two-site polaron problem we know that over a large regime of parameters α and γ the LF approximation gives reliable results as far as the energies of the low lying excitations are concerned. Nevertheless there can be serious discrepancies between the LF approach and the exact results when considering the eigenstates of the polaron problem. Let us illustrate these discrepancies in such physical quantities as

- i) the kinetic energy of the electrons,
- ii) the occupation number of electrons as a function of wave vector,
- iii) the wave vector dependence of the spectral function measurable by angle resolved photoemission experiments,
- iv) the importance of renormalization of the phonon frequencies and of the electron hopping integral
- v) the retardation between the dynamics of the charge carriers and of the lattice deformation which accompanies them.

Let us start by considering the static correlation function $t_{eff}/2t = -E_{kin}/2t \equiv \langle c_{1\sigma}^\dagger c_{2\sigma} \rangle$ which describes the kinetic energy in units of $2t$ and which in the extreme polaronic LF limit (Eq.(10)) becomes t_{LF}^*/t for single polaron hopping and $t_{LF}^{*2}/2\varepsilon_p t$ if it is bipolarons which hop. It is for this reason that sometimes this correlation function is associated with some effective hopping integral $t_{eff}/2t$ which also in the limit $\alpha \Rightarrow 0$ is physically meaningful since it tends to the free electron value equal to $\frac{1}{2}$. Apart from these extreme limits, we shall see below, the interpretation of this correlation function in terms of an effective hopping integral has to be modified. Evaluating this correlation function for the two-site polaron problem by exact diagonalization of the Hamiltonian Eq.(1) we notice that, as a function of α and γ , the exact result for $E_{kin}/2t$ in general strongly deviates from the extreme polaronic LF limiting behavior. We can hence not expect that the LF approximation is applicable even in conjunction with perturbative corrections in terms of $1/\lambda$.

In Fig.(1a) we plot $t_{eff}/2t$ as a function of α for different adiabaticity parameters γ . At a first glance we get the impression that upon going towards the extreme anti-adiabatic limit i.e. $\gamma \rightarrow 0$ and for a fixed value of α we approach the extreme polaronic LF behavior. Yet as can be seen from Fig.(1b) and contrary to a well established belief on this matter, the LF result is approached slower and slower for a fixed $\gamma \ll 1$ as α gets bigger and bigger. These discrepancies with the LF results are not only quantitative but are qualitative in nature as shows the γ dependence of $t_{eff}/2t$. The reason for this qualitatively different behavior lies in the LF approach itself which considers the electrons to be in localized states of the form given by Eq.(9) in which practically the entire charge of the electron and entire deformation of the molecules remains restricted to the molecular site on which the electron sits. This leads to $t_{eff}/t = t_{LF}^*/t = {}_0\langle\Phi(X - X_0)|\Phi(X + X_0)\rangle_0$ at zero temperature which noticeably differs from

$$t_{eff}/t = {}_0^+\langle\Psi(X)|\Psi(X)\rangle_0^- \quad (11)$$

where $|\Psi(X)\rangle_m^\pm$ denote the exact eigenstates which replace $|\Phi(X \pm X_0)\rangle_m$ in the expressions for the LF approximated eigenstates given by Eq.(9). As can be seen from Fig.(2) the exact eigenfunctions $\Psi_m^\pm(X)$, corresponding to the exact eigenstates $|\Psi(X)\rangle_m^\pm$, differs significantly from the LF approximated eigenfunctions $\Phi_m^\pm(X)$ which for the groundstate becomes

$$\Phi_0^\pm(X) = \left(\frac{M\omega_0}{\hbar\pi}\right)^{\frac{1}{4}} \exp[-(X \pm X_0)^2(M\omega_0/\hbar)] \quad (12)$$

In contrast to $\Phi_0^\pm(X)$ the exact eigenfunctions $\Psi_0^\pm(X)$ show a substantial deformation of the molecule adjacent to the one where the electron actually sits. This is born out in the smaller of the two peaks of $\Psi_0^-(X)$ for negative values of $\xi \equiv X\sqrt{M\omega_0/\hbar} \simeq -X_0\sqrt{M\omega_0/\hbar}$. It is the presence of this second peak which gives rise to a substantial increase in the value of t_{eff}/t over the LF approximated t_{LF}^*/t . As the coupling strength increases the value of X_0 increases roughly linearly with α . This leads to a separation of the two main peaks of $\Psi_0^+(X)$ and $\Psi_0^-(X)$ respectively, which results in an exponentially small overlap of them. On the contrary the overlap of the main peak of $\Psi_0^+(X)$ with the secondary peak of $\Psi_0^-(X)$

is of order unity since the weight of the secondary peak depends only weakly on the value of α . Since this second contribution to t_{eff}/t always remains much bigger than the first one, we can thus never hope to recuperate the LF result t_{LF}^*/t for whatever fixed value of $\gamma < 1$.

The behavior of the oscillator wavefunction expresses a dynamical delocalization of the polaronic state which has been realized a long time ago and for which variational calculations have given rather satisfactory results for the groundstate (see for instance ref [3]). From the above study of $t_{eff}/2t$ and of the oscillator wave function $\Psi_0^\pm(X)$ it becomes clear that in general effects of dynamical delocalization of the electron cannot be obtained by perturbative expansions in terms of $1/\lambda$ around the LF approximated oscillator wave function, even in the extreme antiadiabatic limit $\gamma \ll 1$. Our findings suggest that it is energetically favorable for the polaron to be partially delocalized and to transfer its charge by multiple hopping processes because it is that which gives rise to the monotonically increasing behavior of t_{eff}/t as a function of γ . These multiple hopping processes play, as we shall see in section 5, an important role in the correlated charge - deformation dynamics of the polaron problem.

As concerns t_{eff}/t for the two electron two-site system we notice from Fig.(3a) a behavior similar to that for the one electron problem. However as can be seen from Fig.(3b), in contrast to the one electron problem, for two electrons it varies linearly with γ which is an indication that it is bipolarons rather than polarons which hop. As γ increases, t_{eff}/t tends towards a constant equal to $\frac{1}{2}$ which is indicative of uncorrelated hopping of the two electrons in the system. There is a significant difference in slope of this correlation function calculated exactly and of that determined by the LF approach. Again, for reasonable parameters where small bipolarons are stable (such as $\alpha = 1.2$ and $\gamma \sim 1$) we find that the exactly calculated correlaton function is orders of magnitude bigger than its LF expression for the same parameters.

In concluding this section we want to point out that although polarons as well as bipolarons exist over a large regime of parameters α and γ , their description in terms of the standard LF approach is generally invalid not only in the physically interesting regime (which lies outside the extreme strong coupling antiadiabatic limit $\gamma \ll 1$) but particularly

in that limit, for which it largely overestimates the degree of self-trapping. The failure of calculating $t_{eff}/2t$ qualitatively correctly within the LF approach was already recognized by Fehske et al. [15] who attributed it to the zero-phonon approximation, inherent in the substitution Eq.(10). They showed [14] that the distribution of the weights of the N phonon state in the ground state shift its maximum to higher values of N with increasing values of $\varepsilon_p/t = 2\alpha^2\gamma$. For a fixed values of α the maximum of this distribution shifts to higher and higher value of N as γ decreases, thus rendering the zero-phonon approximation less and less justified. In order to visualize this behavior we plot this distribution $P(n) = \sum_{N_X=0}^N (|\alpha_{0N_X}^+|^2 + |\alpha_{0N_X}^-|^2) |\beta_{0N-N_X}|^2$ as a function of N for a set of values of α (Fig.4(a)) and of γ (fig.4(b)). From Fig.4(b) we can see from a comparison of the LF approximated distribution with the exact one for a particular choice of $\alpha = 1.2$ how the LF approach overestimates the the self-trapping, with a maximum in $P(N)$ occuring at a significantly higher value of N than is the case in the exactly calculated $P(N)$.

The findings of this section moreover suggest that the effect of dynamical delocalization of the charge carriers in polaronic systems leads to a strengthening the phase coherence of polaronic states. If this is so, then we expect that for a given set of parameters α and γ , states described by the LF approach become unstable, i.e., have their spatial phase coherence destroyed as the temperature increases, while the exact states will maintain this phase coherence up to much higher temperatures. The key to this question lies in the wave vector dependence of the one particle spectral function which will be discussed in the next section and of the occupation number $n_\sigma(k) = \langle c_{k\sigma}^\dagger c_{k\sigma} \rangle$ of the electronic charge carriers. Evaluating $n_\sigma(k)$ for the two lowest eigenstates within the LF approach, that is to say with respect to the two eigenstates given in Eq.(9) with $m = n = 0$ we obtain $n_\sigma(k = 0)_+ = n_\sigma(k = \pi)_- = \frac{1}{2}(1 + \exp(-\alpha^2))$ and $n_\sigma(k = \pi)_- = n_\sigma(k = 0)_+ = \frac{1}{2}(1 - \exp(-\alpha^2))$ respectively. This inversion of the occupation numbers between the ground state and the first excited state leads to the result that at low temperatures (bigger than the difference in energy of the two lowest levels but small compared to the phonon frequency ω_0) $n(k) = \frac{1}{2}$, independent on the wavevector k and thus identical to the result for localized polarons, i.e.

for $t = 0$. Evaluating $n_\sigma(k = 0, \pi)_\pm$ exactly we see from Fig.(5) that the exact result differs from that of the LF approach qualitatively with $n_\sigma(k = 0)_\pm$ not only being larger than $n_\sigma(k = \pi)_\pm$ for the ground state but also for the first excited state, provided $\alpha > \alpha_{cr}(\gamma)$ with $\alpha_{cr}(\gamma)$ increasing monotonically as γ decreases. $\alpha_{cr}(\gamma)$ is determined by that value of α for which t_{eff}/t in Fig. 1(b) tends to the saturation value $\frac{1}{2}$, given by the free electron limit, for a given value of γ . It is this fact which gives the polaron a stronger dynamical coherence than what we would expect on the basis of the LF approach and which shows up in the temperature variation of the effective polaron hopping integral t_{eff} , illustrated in Fig.(6). We notice that in the weak coupling regime ($\alpha \ll 1$), where the electrons behave as quasi-free charge carriers, t_{eff} decreases with increasing temperature. This is precisely what we expect if the phase coherence of the electron is destroyed by thermal fluctuations. On the contrary, in the polaronic regime ($\alpha \geq 1$) we notice an initial small increase of t_{eff} with increasing temperature (corresponding to a decrease in the kinetic energy of the electrons!) which suggests that the dynamical coherence of the polaron increases with increasing temperature. This holds true for temperatures up to some characteristic temperature above which this coherence is definitely destroyed resulting in a decrease of t_{eff} with increasing temperature. This once more strongly contrasts with the result obtained within a LF approach which treats the polarons in terms of band states and which consequently leads to the well known reduction of $t_{LF}^* = \exp(-2\alpha^2 \coth(\beta\omega_0/2))$ with increasing temperature (see Fig.(6)).

These features are of course quite general and will remain when, instead of studying the two-site polaron problem, one deals with the polaron problem in an infinite lattice of finite dimension. There the LF approach is in fact known to give rise to results which contradict our findings for the two-site polaron problem such as the dependence of the occupation number on the wavevector which, apart from a small step at the Fermi vector, is a flat function throughout the Brillouin zone for zero temperature [16]. For any realistic finite temperature, which clearly would be larger than the difference in energy of the two lowest lying eigenstates of the Hamiltonian Eq.(1) (i.e $\simeq 2t \exp(-2\alpha^2)$), the LF approach thus would

lead one to expect $n_\sigma(k)$ to be equal to $\frac{1}{2}$, independent on k and not to show the slightest anomaly at the Fermi wavevector. Furthermore as concerns the temperature variation of t_{eff} discussed above for the two-site polaron problem one expects also for an infinite lattice a mobility which increases with increasing temperature. The opposite behavior is found in the classical works on that issue and being based on the LF $1/\lambda$ perturbative approach [12,17].

An important feature in polaron physics is the crossover from small polarons in the anti-adiabatic strong coupling limit to large polarons in the adiabatic strong coupling limit. This crossover has been studied in great detail and can be seen most clearly if t_{eff} is plotted as a function of $\varepsilon_p/t = 2\alpha^2\omega_0/t$ [14] rather than as here as a function of α . It turns out that the crossover is rather abrupt in the adiabatic strong coupling limit and becomes more spread out when going to the anti-adiabatic limit.

In the following two sections we shall discuss finer details of polaron dynamics which should show up in the spectral properties and the correlated dynamics of the charge carriers and of the molecular deformations which accompany them.

IV. ITINERANT VERSUS LOCALIZED POLARONS

One of the key questions in the physics of small polarons is how to discern itinerant from localized polarons. In principle the answer to this question should be contained in the one particle density of states, which can be measured by photoemission experiments. Considering this problem within the LF approximation, the polarons are described by band states which are characterized by the total momentum $\kappa = k + q$, where k denotes the momentum of the electron and q that of the deformation which accompanies it. As an illustrative example for the one electron two-site polaron problem this implies that the LF groundstate $|LF\rangle_{00}^+ \equiv |LF\rangle_{\kappa=0}$, given by Eq.(9), can be written as

$$|LF\rangle_{\kappa=0} = \frac{1}{\sqrt{2}} \left(c_0^\dagger |\Phi(X)\rangle_0 + c_\pi^\dagger |\Phi(X)\rangle_\pi \right) |\Phi(Y - Y_0)\rangle_0 \quad (13)$$

where

$$c_{(0,\pi)\sigma}^\dagger = \frac{1}{\sqrt{2}} (c_{1\sigma}^\dagger \pm c_{2\sigma}^\dagger), \quad |\Phi(X)\rangle_{0,\pi} = \frac{1}{\sqrt{2}} (|\Phi(X - X_0)\rangle_0 \pm |\Phi(X + X_0)\rangle_0) \quad (14)$$

Hence the scattering cross-sections

$$\begin{aligned} A_{N\sigma_1, \sigma_2, \dots, \sigma_N}^{(2\sigma)}(k, \omega) &= Im \frac{1}{\pi} \int d\tau \exp(i\omega\tau) {}_N \langle c_{k\sigma}^\dagger(\tau) c_{k\sigma}(0) \rangle_N \theta(\tau) \\ A_{N\sigma_1, \sigma_2, \dots, \sigma_N}^{(1\sigma)}(k, \omega) &= Im \frac{1}{\pi} \int d\tau \exp(i\omega\tau) {}_N \langle c_{k\sigma}(\tau) c_{k\sigma}^\dagger(0) \rangle_N \theta(\tau) \end{aligned} \quad (15)$$

measure the intensity of emitted and absorbed electrons with momentum k and spin σ in a polaronic state containing N electrons with spins $\sigma_1, \sigma_2, \dots, \sigma_N$ in the groundstate.

Let us first consider the case of an isolated polaronic center with one and respectively two electrons present. We shall from now on consider only the case $U = 0$. The two cross-sections, given in Eq.(15), are then exactly determined by

$$\begin{aligned} A_{0, 1\uparrow}^{(1\uparrow, 2\uparrow)}(\omega) &= \sum_{l=0}^{\infty} \exp(-\alpha^2) \frac{\alpha^{2l}}{l!} \delta(\omega - \varepsilon_p \mp l\omega_0) \\ A_{1\uparrow, 2\uparrow\downarrow}^{(1\downarrow, 2\downarrow)}(\omega) &= \sum_{l=0}^{\infty} \exp(-\alpha^2) \frac{\alpha^{2l}}{l!} \delta(\omega - 3\varepsilon_p \mp l\omega_0) \end{aligned} \quad (16)$$

which gives the well known Poisson distribution of the phonon modes locked together in the construction of the coherent Glauber states which define localized polarons. We shall now show that the overall features of these spectral functions are preserved when considering a system of itinerant polarons. For that purpose let us consider the spectral function for electron emission from a one polaron ground state in the two-site polaron problem within the LF approach. We then obtain

$$\begin{aligned} A_{1\uparrow}^{(2\uparrow)}(k=0, \omega)_0 &= \sum_{l \text{ even}}^{\infty} \sum_{l'}^{\infty} \exp(-2\alpha^2) \frac{\alpha^{2(l+l')}}{l!l'} \delta(\omega - \varepsilon_p - (l+l')\omega_0) \\ A_{1\uparrow}^{(2\uparrow)}(k=\pi, \omega)_0 &= \sum_{l \text{ odd}}^{\infty} \sum_{l'}^{\infty} \exp(-2\alpha^2) \frac{\alpha^{2(l+l')}}{l!l'} \delta(\omega - \varepsilon_p - (l+l')\omega_0) \end{aligned} \quad (17)$$

if the system is in the ground state and $A_{1\uparrow}^{(2\uparrow)}(k=0, \omega)_1 (= A_{1\uparrow}^{(2\uparrow)}(k=\pi, \omega)_0)$ and $A_{1\uparrow}^{(2\uparrow)}(k=\pi, \omega)_1 (= A_{1\uparrow}^{(2\uparrow)}(k=0, \omega)_0)$ if it is in the first excited state. This shows that the bulk of the spectrum of itinerant polarons (i.e. $t \neq 0$) is identical to that of localized ones except for the lowest energy part of the spectrum i.e. for small values of l . For that part of the

spectrum the spectral weight for $k = 0$ in the ground state equals $\simeq \exp - (2\alpha^2)$ while it is identically zero for $k = \pi$. The opposite is true for the first excited state. These are precisely the features expected for quasi-particles whose weights for their coherent part is strongly reduced. The exact results of the spectral functions bare this out and in Fig.(7a) we present $A_{1\uparrow}^{(2\uparrow)}(k = 0, \omega)_0$ for values of γ and α which characterize well defined polaronic states. In order to compare $A_{1\uparrow}^{(2\uparrow)}(k = 0, \omega)$ with $A_{1\uparrow}^{(2\uparrow)}(\omega)$ for localized polarons (i.e. $t = 0$) as well as with $A_{1\uparrow}^{(2\uparrow)}(k = \pi, \omega)$ we do this for finite rather than zero temperature since for all intents and purposes the level splitting between the first two lowest energy levels (corresponding to the bandwidth $2t^*$ of the coherent polaron motion) is extremely small, since under normal conditions we are dealing with temperatures T such that $2t^* \ll k_B T \ll \omega_0$. Under those circumstances the LF approach yields scattering cross-sections $A_{1\uparrow}^{(2\uparrow)}(k, \omega)$ which become wave vector independent and thus undistinguishable from purely localized polarons. The exactly calculated spectral functions become, up to a k dependent scaling factor, practically identical with $A(\omega)$ for the entire frequency regime except for the low frequency part, where however the spectral weight is extremely small (see Fig.7b). These findings suggest that small polarons might never exist in form of coherent Bloch like states, a feature which is supported by the dynamics of the polaron motion, which will be discussed in section V.

One of the prime problems in the physics of the many polaron problem is the question of how to discern a system of essentially non-interacting polarons from one in which they sense a strong attraction between them and which ultimately leads to the formation of tightly bound pairs (bipolarons). In principle this question can be resolved by photoelectron spectroscopy which measures the one particle density of states for polarons. In fact what is required in order to discriminate between a many body ground state containing essentially unpaired from one containing essentially paired polarons is both, photoemission and inverse photoemission spectroscopy. Testing the system with solely photoemission we can not decide about the nature of the many body ground state. This can be illustrated on the basis of the two-site polaron system containing one and respectively two electrons. The scattering cross section looks essentially similar for the two cases. In Fig.(8,a-d) we plot for different values

of coupling strength α the photoemission spectrum $A_{2\uparrow\downarrow}^{(2\uparrow)}(k=0, \omega)$ where an electron is emitted out of a two-electron two-site polaron system. This spectrum has the same form as $A_{1\uparrow}^{(2\uparrow)}(k=0, \omega)$ (see Fig.(7a)) which corresponds to the situation of an electron emitted out of a one-electron two-site system. On the contrary, the inverse photoemission spectrum can clearly distinguish if the final state corresponds to a state with essentially uncoupled polarons or polaron pairs. Looking at this spectral function for the one-electron two-site system i.e., $A_{1\uparrow}^{(1\downarrow)}(k=0, \omega)$ we see from Fig.(9a-d) that, as we increase the coupling strength, a two peak structure emerges. The energy gap which separates this two peak structure amounts to $2\varepsilon_p$, which represents precisely the binding energy between two polarons in the strong coupling limit. The low energy peak of this spectrum corresponds to a final state given by a bipolaron in its bonding singlet state, having energy $\simeq 4\varepsilon_p$. The high energy peak arises from a bipolaronic state in its antibonding singlet and respectively triplet state having an energy $\simeq 2\varepsilon_p$ [18]. The difference in energy between these two contributions in the spectral function for inverse photoemission is hence just the binding energy of a bipolaron and thus can serve as a signature for a bipolaronic many polaron ground state.

It is even moreover illustrative to study the one particle density of states for those situations. In Figs.(10,a-d) we plot the density of states per spin for the one electron two-site system at zero temperature

$$\rho_1(\omega) = \sum_{k=0,\pi} \left(A_{1\uparrow}^{(2\uparrow)}(k, \omega)_0 + A_{1\uparrow}^{(1\uparrow)}(k, \omega)_0 \right) \quad (18)$$

as a function of coupling strength α and for a given fixed value of adiabaticity parameter $\gamma = 1.1$. For small values of α the density of states is characterized by two peaks centered around energies $\omega \simeq 0$ and $\omega \simeq 2t$, which in essence represents quasi free electrons in the bonding and respectively anti-bonding states for this small system. As α increases these two peaks spread and eventually evolve into two well separated peaks. This density of states is similar to that of the Hubbard model in the dilute limit (i.e., far away from half filling) which shows indications for the presence of an upper and a lower Hubbard band, separated by the Hubbard U repulsion energy, but without any clear gap between those two bands.

Similarly to the Hubbard problem, the two peaks in the polaron problem are separated by the energy of attraction between two polarons, which in case of strong coupling (such as illustrated in Fig.(9d) for $\alpha = 2.2$) amounts to $2\varepsilon_p$.

A similar density of states per spin is obtained for the two electron two-site system

$$\rho_2(\omega) = \sum_{k=0,\pi} \left(A_{2\uparrow\downarrow}^{(2\uparrow)}(k, \omega)_0 + A_{2\uparrow\downarrow}^{(1\uparrow)}(k, \omega)_0 \right) \quad (19)$$

which we illustrate in Figs.11(a-d) as a function of coupling strength α and for a given fixed value of adiabaticity parameter $\gamma = 1.1$. We again see a similar evolution of the density of states as we increase α but now the separation in energy is equal to $4\varepsilon_p$, which can be clearly distinguished from the case representative for uncoupled polarons (the one electron two site problem considered above). A clear energy gap given by $2\varepsilon_p$ now appears separating the low and high frequency peak structures. Integrating $\rho_2(\omega)$ up to some value $\omega = \varepsilon_F$ such that it becomes equal to 2 (which corresponds to the half filled band case and to two electrons in our system) we find that ε_F lies precisely in the middle of the gap of the density of states. This again is reminiscent of the problem of strongly correlated electrons for the half filled band Hubbard model. These features examined here for the two-site polaron system are expected to hold true generally for any interacting many polaron system on a lattice.

V. CORRELATED CHARGE-DEFORMATION DYNAMICS

The polaron problem presents a highly non-linear dynamical system in which the charge and deformation fluctuations are intricately coupled together. This leads to a dynamics of the molecular deformations being driven by the dynamics of the charge carriers in the strong coupling anti-adiabatic regime ($\alpha \gg 1, \gamma \ll 1$). On the contrary it is the dynamics of the molecular deformations which drives the dynamics of the charge carriers in the weak coupling adiabatic regime ($\alpha \ll 1, \gamma \gg 1$). In general this leads to a dynamics for the charge and of the molecular deformations which is composed of a common slow oscillation and fast ones superposed on it. The fast oscillations for the charge dynamics have a frequency \tilde{t} of

the order of t , while those for the deformation dynamics have a frequency $\tilde{\omega}_0$ which is of the order of ω_0 .

In this section we shall study the evolution of those dynamical properties of small polarons when we go from the strong coupling anti-adiabatic regime to the strong coupling adiabatic one, with a special emphasis on the behavior in the crossover regime. In order to illustrate this behavior we evaluate the time dependent correlation functions for the charge redistribution and molecular deformations:

$$\chi_{nm}(\tau) = \langle (n_{1\sigma}(\tau) - n_{2\sigma}(\tau))(n_{1\sigma}(0) - n_{2\sigma}(0)) \rangle, \quad \chi_{xx}(\tau) = \langle X(\tau)X(0) \rangle \quad (20)$$

In Figs.12(a-d) we plot these correlation functions (normalized with respect to their $\tau = 0$ values) as a function of time τ in units of ω_0 for different values of the γ and fixed α . We notice that the charge dynamics qualitatively tracks globally the behavior expected on the basis of the LF approximation in the anti-adiabatic limit (i.e., for $\gamma = 0.1$, Fig.12(a)) but with superposed small amplitude fast charge oscillations with a frequency \tilde{t} which is large compared to the unrenormalized electron hopping integral t . The dynamics of the molecular deformation follows in a coherent fashion that of the charge and exhibits superposed molecular vibrations with a frequency $\tilde{\omega}_0 \simeq \omega_0$. As we increase γ (i.e., for $\gamma = 1.1$, Fig.12(b)), the amplitude of the fast charge oscillations become increasingly important and their oscillation frequency \tilde{t} decreases. The opposite behavior is obtained for the molecular deformation oscillations, whose frequency $\tilde{\omega}_0$ of the fast oscillatory behavior increases while the corresponding amplitude diminishes. The system is then no longer described by the LF approach (as we can see from the comparison made for this case) and the charge dynamics is now controlled by multiple hopping processes with concomitantly reduced amplitude fluctuations of the molecular deformations. Upon further increasing γ we arrive at a situation where the frequencies and amplitudes of those two dynamical variables, characterizing the charge and deformation, become comparable to each other i.e., for $2\tilde{t} \simeq \tilde{\omega}_0$ and we enter the crossover regime (i.e., for $\gamma = 1.6$, Fig.12(c)). This regime is characterized by a temporarily alternating behavior between essentially self-trapped anti-adiabatic small polarons (manifest in a

substantial reduction of the amplitude fluctuations of the charge dynamics) and a behavior reminiscent of itinerant adiabatic polarons as seen upon a further increase of γ (ie., $\gamma = 2.0$, Fig.12(d)). Such fluctuations in the amplitudes of the charge occur over a time scale which is large compared to the inverse hopping rate \tilde{t} and is accompanied by phase slips in the fast oscillatory behavior of the charge as well as the deformation fluctuations.

The evolution of the correlation functions for the charge and deformation fluctuations of the two-electron two-site problem as a function of the adiabaticity parameter γ and fixed coupling constant α follows a similar behavior to that of the one-electron two-site problem, as shown in Figs.13(a-d). Again we can identify a crossover between small bi-polarons and essentially uncorrelated two electrons which occurs for $\gamma \simeq 1.3$ for the particular choice $\alpha = 0.6$

This crossover between self-trapped polarons, respectively bi-polarons, and quasifree electrons in the phase space of α and γ corresponds to the characteristic value of γ where the kinetic energy of the electrons $E_{kin} = -2t\langle c_{1,\uparrow}^\dagger c_{2,\uparrow} \rangle$ approaches its maximal value of the free electron limit, while the potential energy of the electrons $E_{pot} = -2\lambda\langle (n_{1,\uparrow} + n_{1,\downarrow})u_1 \rangle$ tends to its minimum value $-\frac{1}{\sqrt{2}}\lambda Y_0\langle (n_{1,\uparrow} + n_{1,\downarrow}) \rangle$, obtained in the limit $\gamma \Rightarrow \infty$. This can be seen from the behavior of E_{kin} illustrated in Fig.1(b) and of E_{pot} depicted in Fig.14 for $\alpha = 1.2$ and $\gamma \simeq 1.6$ for the one-electron two-site problem. The crossover between self-trapped small polarons and quasi-free electrons thus appears to be driven by a competition between the kinetic and potential energy of the electrons; the first one favoring a delocalization of them while the second one inciting them to localize on the molecular sites. In an infinite solid state system such a scenario would suggest a quantum phase transition between a metal and a polaronic insulator as proposed a long time ago by Landau and Froehlich [20]. For systems with low carrier concentrations such localized polarons have been verified experimentally in metal halide where optically excited excitons get localized [21]. There is at present no exact theorem as to whether pure electron phonon-systems can show such a polaronic insulator. The present exact proofs against that [22] hinge on suppositions of the phonon spectra which may not be realistic for real materials.

We finally should like to point out that no significant changes in the phonon distribution of the displaced oscillators are observed when going through this crossover regime. This can be verified from the plot in Fig.4(b) of $P(N)$ for a fixed $\alpha = 1.2$ and upon varying γ .

In Table I we summarize our findings on the charge-deformation dynamics of a polaronic system. We compare for that purpose the renormalized vibrational frequency $\tilde{\omega}_0$, the renormalized electron hopping integral \tilde{t} , the kinetic energy of the electrons t_{eff}/t and the physical charge transfer rate t^* for different values of the adiabaticity parameter γ and for a fixed coupling constant α . In the limit of strong adiabaticity, t^* tends to the LF value t_{LF}^* and follows as a function of γ the behavior of $(E_1 - E_0)/2$ which denotes the difference in energy of the two lowest eigenstates. We also indicate the spectral weight Z of the lowest energy contribution to the scattering cross-section and notice that for the anti-adiabatic limit it scales with t^*/t . This is an indication that the low frequency part of the scattering cross-section corresponds to coherent states but with a spectral weight which is extremely small. It is presently not clear whether such weak coherent features, characteristic of itinerant small polarons, will persist if one treats the polaron problem on a infinite lattice. Calculations based on infinite dimensions [23] which show such itinerant behavior do neglect totally the frequency renormalization of the vibrational motion of the atoms, which we consider as the prime cause for dephasing of the correlated charge-deformation dynamics and ultimately believed to be responsible for the destruction of itinerant polaronic states.

The strong coupling between the charge and the molecular deformations thus manifests itself not only in a strong renormalization of the molecular vibrational frequency ω_0 becoming $\tilde{\omega}_0$ but also in a strong renormalization of the intrinsic hopping integral t renormalized into \tilde{t} . As we go from the anti-adiabatic limit toward the adiabatic one (for fixed value of α), we observe a substantial decrease in \tilde{t}/t and a concomitant increase in $\tilde{\omega}_0$. These are effects which should be observable by spectroscopic measurements such as infrared or Raman scattering for the vibrational modes.

From inspection of Figs.(12,13) we notice the sizeable dynamical delocalization of the

polaron and bi-polaron respectively as we approach the crossover regime. In the crossover regime itself this delocalization alternates between partly quasi-static delocalization, suggesting almost localized yet extended polaron states and dynamical delocalization reminiscent of almost free carriers, which however remain dynamically tied to a given molecule for some appreciable time. To be more specific, for the particular case illustrated in Fig.12(c), we find for the period of time when a quasi-static polaron is stable, a charge distribution given by: $\langle n_{1,\sigma} \rangle \simeq 0.75$ and $\langle n_{2,\sigma} \rangle \simeq 0.25$. On the other hand for the dynamically delocalized polaron we find that the charge distribution fluctuates over a characteristic time given by \tilde{t} between $\langle n_{1,\sigma} \rangle \simeq 1.0$, $\langle n_{2,\sigma} \rangle \simeq 0$ and $\langle n_{1,\sigma} \rangle \simeq 0.5$, $\langle n_{2,\sigma} \rangle \simeq 0.5$. Such temporal fluctuations were initially hypothesized by us a long time ago [19] which led to the Boson-Fermion model for intermediary coupling electron phonon systems, which may have some relevance for our understanding of High T_c superconductors [24,25].

VI. SUMMARY

The main objective of this work was the study of the intricate dynamics of the polaron problem involving the dynamical behavior of the charge carriers and that of the molecular deformations which surround them. We find that in the anti-adiabatic regime for small polarons the molecular deformations follow in a coherent fashion the redistribution of the charge, while in the adiabatic regime it is the charge redistribution which follows the molecular deformations. In the crossover regime between those two limiting cases we find that the dynamical behavior of the polaronic charge carriers alternates between self-trapped polarons and almost free carrier behavior. The time scale over which these different behaviors are realized is typically an order of magnitude bigger than the intrinsic hopping rate i.e., of the order $10 \times 2\pi/t$. This crossover regime is characterized by strong renormalization of the intrinsic hopping integral as well as of the bare phonon frequency, which in this regime become equal. Phase slips in the fast oscillatory components of the charge and molecular deformation fluctuations are the result of this. Such effects are expected to be essential

for a proper description of polaron damping, so far having been treated only within the LF approach [26], and which is unable to account for the effects described here.

The question of how to distinguish itinerant polarons from localized ones was studied here on the basis of the one particle spectral function and its temperature dependence. We showed that at zero temperature the respective spectral functions for localized and itinerant polarons differ from each other only very slightly except for the low frequency regime of the spectral function, where they show an increased spectral weight for small wave vectors if the polarons are itinerant. As the temperature increases this difference disappears and it is, in principle, no longer possible by spectroscopic means to distinguish between localized and itinerant small polarons. This may explain the puzzling results in the photoemission spectra for certain High T_c superconducting cuprates for which a wave vector independent spectral function was observed in the normal state and consequently was interpreted as indications for localized charge carriers [27]. The question of a polaronic insulator versus a polaronic metal has been touched upon here only from the point of view of the single particle properties. The polaron problem is however presents a problem of electrons in a system with impurity centers with dynamically varying energies and thus contains features similar to those of the Anderson localization. The relevant quantity to be studied hence is the conductivity. So far a few attempts in this direction have been made on the basis of exact diagonalization studies in finite systems [28] attempting to determine whether there is or not a finite Drude component in the optical conductivity.

Finally, our exact diagonalization studies on the two-site molecular Holstein polaron model permitted us to discuss the limitations of the standard LF approach. Our rather unexpected and perhaps widely unrecognized findings are that this approach, which is generally believed to become exact in the limit of anti-adiabaticity and an electron phonon coupling going to infinity, actually diverges most from the exact results precisely in this limit. The reasons for that can be traced back to the zero-phonon approximation inherent in the LF approach, based on the relation Eq. (10) and which, with increasing coupling strength, is increasingly strongly violated [15].

Our analysis of the various spectral functions and the density of states shows that the major part of the spectrum must be considered as being due to incoherent rather than coherent polaron dynamics; the latter having vanishingly small spectral weight of order $\exp(-2\alpha^2)$. This result confirms our earlier findings on the many polaron problem for infinite lattices [29] and examinations of the single polaron problem in infinite dimensions [23].

VII. ACKNOWLEDGEMENT

We are indebted to S. Ciuchi, H.Fehske and J.M.Robin for many valuable discussions and J.M.R. for making available to us certain of his independently derived results on the evaluation of the spectral functions. E.V.L.M. acknowledges a post doctoral fellowship from the Brazilian council for national Research (*CNPq*).

† On leave of absence from the Departamento de Física, Universidade Federal Fluminense, Rio de Janeiro, Brazil.

REFERENCES

- [1] H.de Raedt and Ad. Lagendijk, Phys.Rev.B **27**, 6097 (1983).
- [2] I.J.Lang and Yu.A. Firsov, Sovjet Physics JETP **16**,1301 (1962).
- [3] H.B.Shore and L.M.Sander, Phys.Rev.B **7**,4537 (1973).
- [4] P.Prelovsek, J. Phys. C **12**,1855 (1979).
- [5] S.Weber and H. Buettner, Solid State Comm., **56**, 395 (1985).
- [6] F.de Pasquale, S. Ciuchi, J.Bellisard and D.Feinberg, Reviews of Solid State Science, **2**,443 (1988).
- [7] C.R.Proeto and L.M.Falikov, Phys.Rev.B **39**, 7545 (1989).
- [8] F.Marsiglio, Phys.Lett.A **180**,280 (1990).
- [9] J.Ranninger and U.Thibblin, Phys. Rev.B **45**, 7730 (1992).
- [10] A.S.Alexandrov, V.V.Kabanov and D.K.Ray, Phys.Rev.B **49**,9915 (1994).
- [11] J.M.Robin, cond-mat/9610219.
- [12] Yu.A.Firsov, Polarons (Moskow, Nauka,1975); ibid. Semiconductors **29** 515 (1995).
- [13] A.S.Alexandrov and J.Ranninger, Phys.Rev.B. **23**, 1796 (1981).
- [14] G.Wellein, H.Röder and H. Fehske, Phys.Rev.B **53**,9666 (1996); W.Stephan, Phys.Rev.B **54**, 8981 (1996).
- [15] H.Fehske, H.Röder, G.Wellein and A.Mistriotis, Phys.Rev. B **51**,16582 (1995).
- [16] J.Ranninger, Phys. Rev.B **48**, 13166 (1993).
- [17] T. Holstein, Ann.Phys.(NY) **8**,343 (1959).
- [18] This corrects our earlier results in ref([9]) in which certain contributions to these correlation functions were inadvertently omitted.

- [19] J.Ranninger and S.Robaszkiewicz, *Physica B* **135**, 468 (1985).
- [20] L.D.Landau, *Sov.Phys.***3** 644 (1933), H.Froehlich, *Proc.Phys.Soc.A* **160** 230 (1937).
- [21] M.Ueta, H.Kanzaki, K.Kobayashi, Y.Toyozawa and Hanamura, in "Excitonic Processes in Solids", Springer Series in Solid State Science **60** (Springer, Berlin, 1986).
- [22] B.Gerlach and H. Loewen. *Rev.Mod.Phys.* **63**, 63 (1991), E.H.Lieb and L.E.Thomas, *Comm.Math.Phys.* **183** (1997).
- [23] S.Ciuchi, F.de Pasquale and D. Feinberg, *Europhys. Lett.* **30** 151 (1995).
- [24] J.Ranninger, J.M.Robin and M.Eschrig, *Phys.Rev.Lett.* **74**,4027 (1995).
- [25] J.Ranninger and J.M.Robin, *Phys.Rev.B* **53** R11961 (1996).
- [26] J.Loos, *Z.Phys.B* **92**,377 (1993).
- [27] Jian Ma, C.Quitmann, R.J.Kelley, G.Margaritondo and M.Onellion, *Solid State Commun.* **94** 27 (1995).
- [28] H.Fehske, G.Wellein, B.Baeuml and R.N.Silver *cond-mat* 9612202.
- [29] A.S.Alexandrov and J.Ranninger, *Phys.Rev.B* **45** 13109 (1992).

FIGURES

Fig.1 $t_{eff}/2t = -E_{kin}/2t = \langle c_{1\sigma}^\dagger c_{2\sigma} \rangle$ for a single electron as a function of α for different adiabaticity parameters γ for the two-site polaron problem (a). Comparison of t_{eff}/t evaluated by exact diagonalization and its approximative value given by the LF approach as a function of γ for several values of α (b).

Fig.2 The exact oscillator wave function $\Psi_0^+(\xi)$ with $\xi = X\sqrt{M\omega_0/\hbar}$ for a single electron in the two-site polaron system for different values of α .

Fig.3 t_{eff}/t for two electrons as a function of α for different adiabaticity parameters γ for the two-site polaron problem (a). Comparison of t_{eff}/t evaluated by exact diagonalization with its approximated value given by the LF approach as a function of γ for different values of α (b).

Fig.4 (a) The phonon number distribution $P(N)$ for a given value of $\alpha = 1.2$ and for various values of γ . Notice that as γ decreases, the distribution function tends to that of localized polarons, practically indistinguishable from that of $\gamma = 0.1$. (b) The phonon number distribution for a given value of $\gamma = 1.6$ and for various values of α . Notice the in general significant difference between the LF approximated distribution function and the exact results, illustrated here for $\alpha = 1.2$.

Fig.5 The wave vector dependence of the polaron occupation number $n_\sigma^{pol}(k)_\pm$ for the two lowest lying states. For comparison we also plot the result for the LF approximated states given in Eq.(9).

Fig.6 t_{eff}/t (normalized to its zero temperature value) as a function of temperature (in units of ω_0) for fixed $\gamma = 1.1$ and for different values of α and compared with the LF approach results.

Fig.7 The scattering cross-section $A_{1\uparrow}^{(2\uparrow)}(k = 0, \omega)_0$ for $\gamma = 1.1$ and $\alpha = 2.2$ and for $k_B T = 0.1\omega_0$ (a). Comparison of the scattering cross-sections $A_{1\uparrow}^{(2\uparrow)}(k = 0, \omega)_0$ and $A_{1\uparrow}^{(2\uparrow)}(\pi, \omega)_0$ with each other as well as with that for localized polarons i.e., $A_{1\uparrow}^{(2\uparrow)}(\omega)_0$ for $k_B T = 0.1\omega_0$ and $T = 0$ (b). These scattering cross-sections have been obtained by broadening the set of δ functions by Gaussians of width $\Delta\omega = 0.1\omega_0$.

Fig.8(a-d) The scattering cross-section $A_{2\uparrow\downarrow}^{(2\uparrow)}(k = 0, \omega)_0$ for photoemission from a two electron two-site system as a function of increasing electron phonon coupling α . These scattering cross-sections have been obtained by broadening the set of δ functions by Gaussians of width $\Delta\omega = 0.1\omega_0$.

Fig.9 The scattering cross-section $A_{1\uparrow}^{(1\uparrow)}(k = 0, \omega)_0$ for inverse photoemission from a one-electron two-site system as a function of increasing electron phonon coupling α . The scattering cross-section has been obtained by broadening the set of δ functions by Gaussians of width $\Delta\omega = 0.1\omega_0$.

Fig.10(a-d) The evolution of the density of states $\rho_1(\omega)$ for the one-electron two-site polaron problem as the electron phonon coupling α increases and for a fixed adiabaticity parameter $\gamma = 1.1$. The densities of states have been obtained by broadening the set of δ functions by Gaussians of width $\Delta\omega = 0.1\omega_0$.

Fig.11(a-d) The evolution of the density of states $\rho_2(\omega)$ for the two-electron two-site polaron problem as the electron phonon coupling α increases and for a fixed adiabaticity parameter $\gamma = 1.1$. The densities of states have been obtained by broadening the set of δ functions by Gaussians of width $\Delta\omega = 0.1\omega_0$.

Fig.12a χ_{nn} and $\chi_{xx}(t)/\langle X^2 \rangle$ for $\alpha = 1.2$ and $\gamma = 0.1$ for the one-electron two-site polaron system.

Fig.12b χ_{nn} and $\chi_{xx}(t)/\langle X^2 \rangle$ for $\alpha = 1.2$ and $t\gamma = 1.1$ for the one-electron two-site polaron system.

Fig.12c χ_{nn} and $\chi_{xx}(t)/\langle X^2 \rangle$ for $\alpha = 1.2$ and $\gamma = 1.6$ for the one-electron two-site polaron system.

Fig.12d χ_{nn} and $\chi_{xx}(t)/\langle X^2 \rangle$ for $\alpha = 1.2$ and $\gamma = 2.0$ for the one-electron two-site polaron system.

Fig.13a χ_{nn} and $\chi_{xx}(t)/\langle X^2 \rangle$ for $\alpha = 0.6$ and $\gamma = 0.2$ for the two-electron two-site polaron system.

Fig.13b χ_{nn} and $\chi_{xx}(t)/\langle X^2 \rangle$ for $\alpha = 0.6$ and $\gamma = 0.8$ for the two-electron two-site polaron system.

Fig.13c χ_{nn} and $\chi_{xx}(t)/\langle X^2 \rangle$ for $\alpha = 0.6$ and $\gamma = 1.3$ for the two-electron two-site polaron system.

Fig.13d χ_{nn} and $\chi_{xx}(t)/\langle X^2 \rangle$ for $\alpha = 0.6$ and $\gamma = 1.6$ for the two-electron two-site polaron system.

Fig.14 Comparison of the electronic kinetic and potential energy $E_{pot} = -2\lambda\langle(n_{1,\uparrow} + n_{1,\downarrow})u_1\rangle$ (as a function of γ for a fixed $\alpha = 1.2$ for the one-electron two-site problem. The crossover regime between self-trapped polarons and quasi-free electrons occurs when the kinetic energy tends to its maximal value while that of the potential energy tends to its minimal value.

TABLES

$\gamma = t/\omega_0$	\tilde{t}/t	$\tilde{\omega}_0/\omega_0$	$\tilde{t}/\tilde{\omega}_0$	t_{eff}/t	$\Delta E/2t$	t^*/t	Z
0.1	-	1.03	-	$1.00 \cdot 10^{-1}$	$5.65 \cdot 10^{-2}$	$5.61 \cdot 10^{-2}$	$6.11 \cdot 10^{-2}$
0.3	5.66	1.08	1.57	$1.90 \cdot 10^{-1}$	$5.73 \cdot 10^{-2}$	$5.66 \cdot 10^{-2}$	$7.25 \cdot 10^{-2}$
0.5	3.05	1.14	1.34	$2.82 \cdot 10^{-1}$	$5.95 \cdot 10^{-2}$	$5.98 \cdot 10^{-2}$	$8.59 \cdot 10^{-2}$
1.1	1.56	1.42	1.21	$5.64 \cdot 10^{-1}$	$6.98 \cdot 10^{-2}$	$6.79 \cdot 10^{-2}$	$1.34 \cdot 10^{-1}$
1.3	1.41	1.52	1.07	$6.20 \cdot 10^{-1}$	$7.63 \cdot 10^{-2}$	$6.90 \cdot 10^{-2}$	$1.49 \cdot 10^{-1}$
1.6	1.25	-	-	$7.12 \cdot 10^{-1}$	$7.84 \cdot 10^{-2}$	$7.85 \cdot 10^{-2}$	$1.70 \cdot 10^{-1}$
1.7	1.28	-	-	$7.38 \cdot 10^{-1}$	$7.97 \cdot 10^{-2}$	$8.03 \cdot 10^{-2}$	$1.75 \cdot 10^{-1}$
2.0	1.19	-	-	$8.00 \cdot 10^{-1}$	$8.26 \cdot 10^{-2}$	$8.26 \cdot 10^{-2}$	$1.90 \cdot 10^{-1}$

TABLE I. The variation of the renormalized frequency of the deformation oscillations $\tilde{\omega}_0$ and of the renormalized hopping rate \tilde{t} as a function of the adiabaticity parameter γ for fixed coupling constant $\alpha = 1.2$. Notice that as we approach the crossover regime, the time scales of these two oscillations become equal i.e., $\tilde{t}/\tilde{\omega}_0 \rightarrow 1$. We also compare the frequency t^* of the slow polaronic motion with the splitting of the two lowest eigenvalues $\Delta E/2t$ and t_{eff} (the electron kinetic energy). Notice that the spectral weight Z of the lowest frequency pole of the electron Green's function scales fairly well with the renormalization factor for the polaron bandwidth t^*/t .

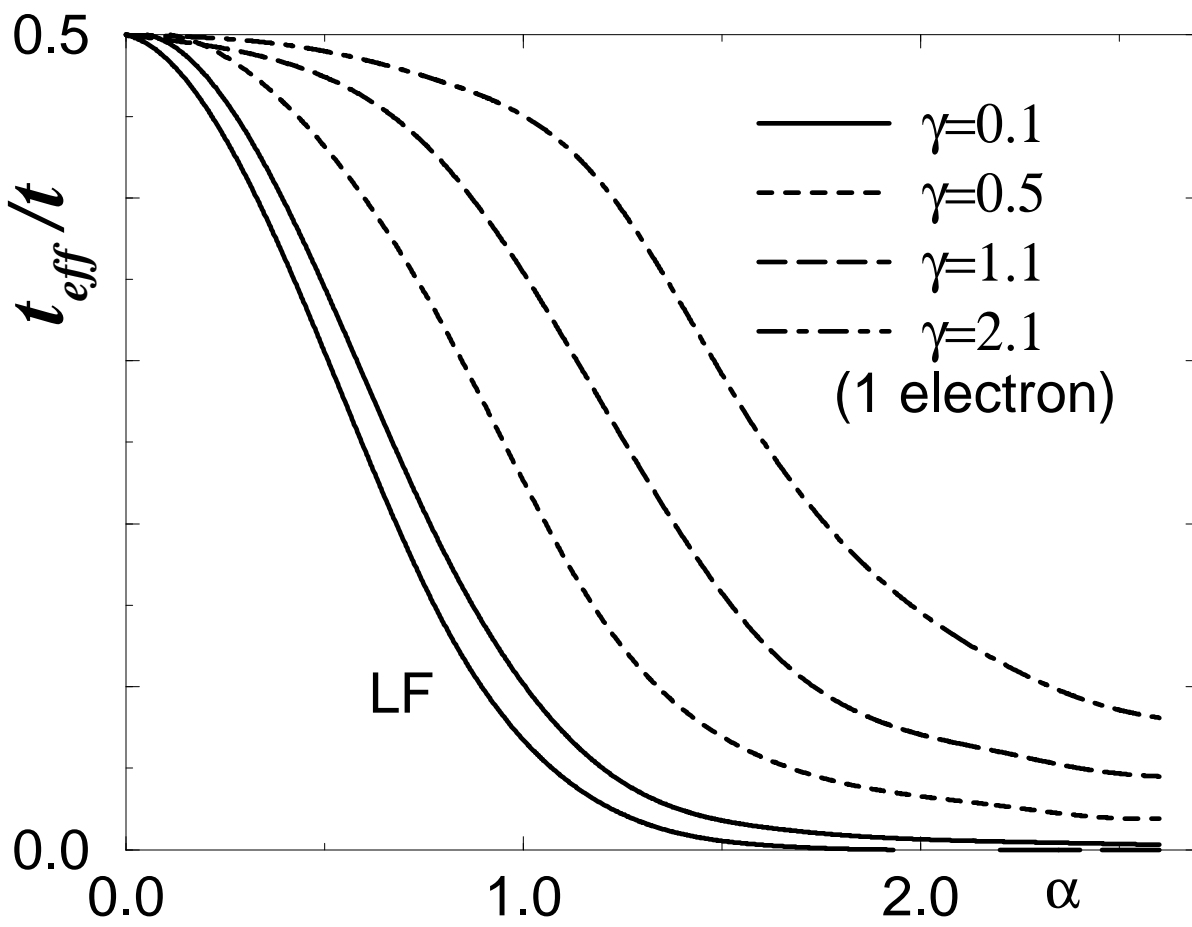


Fig.1a

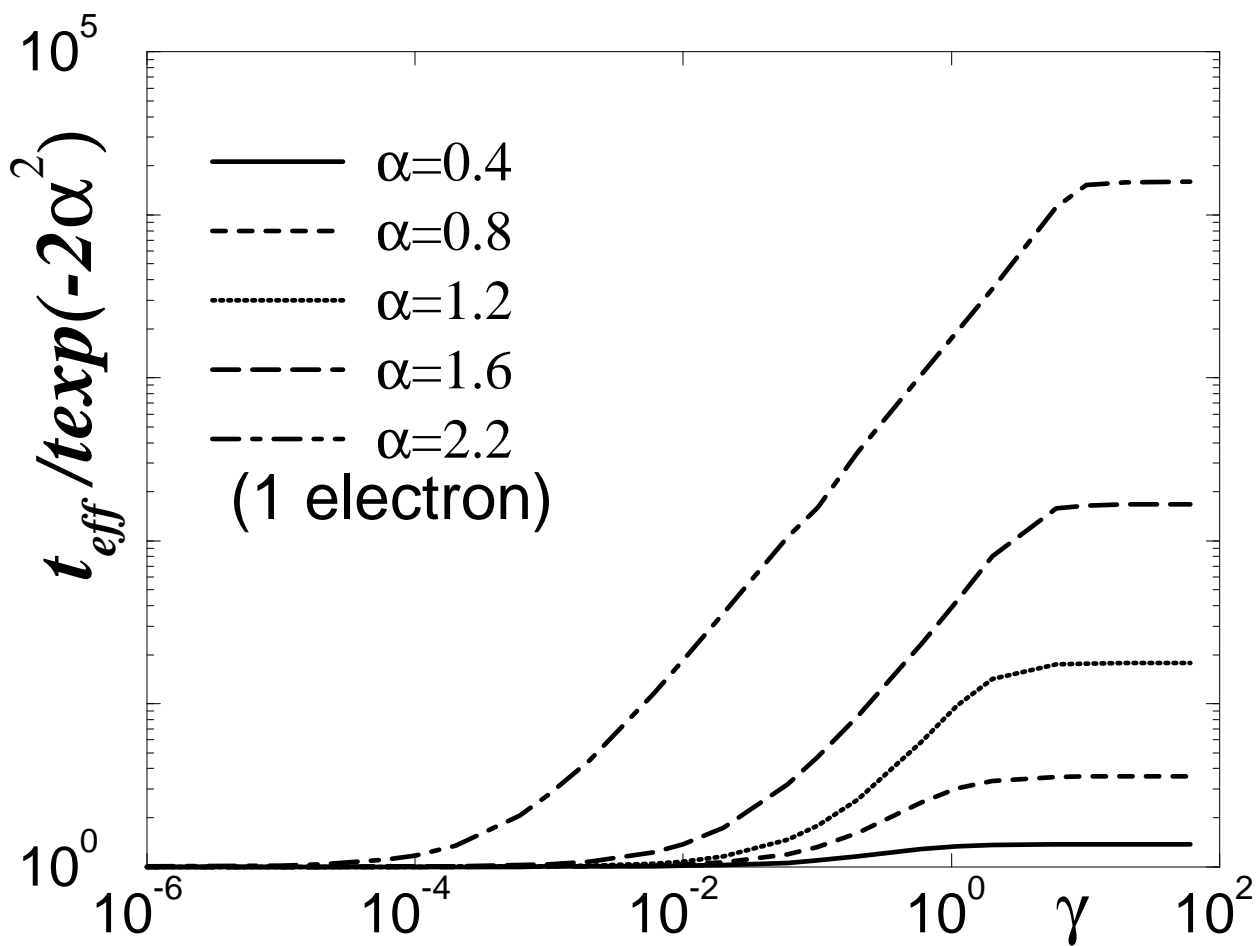


Fig.1b

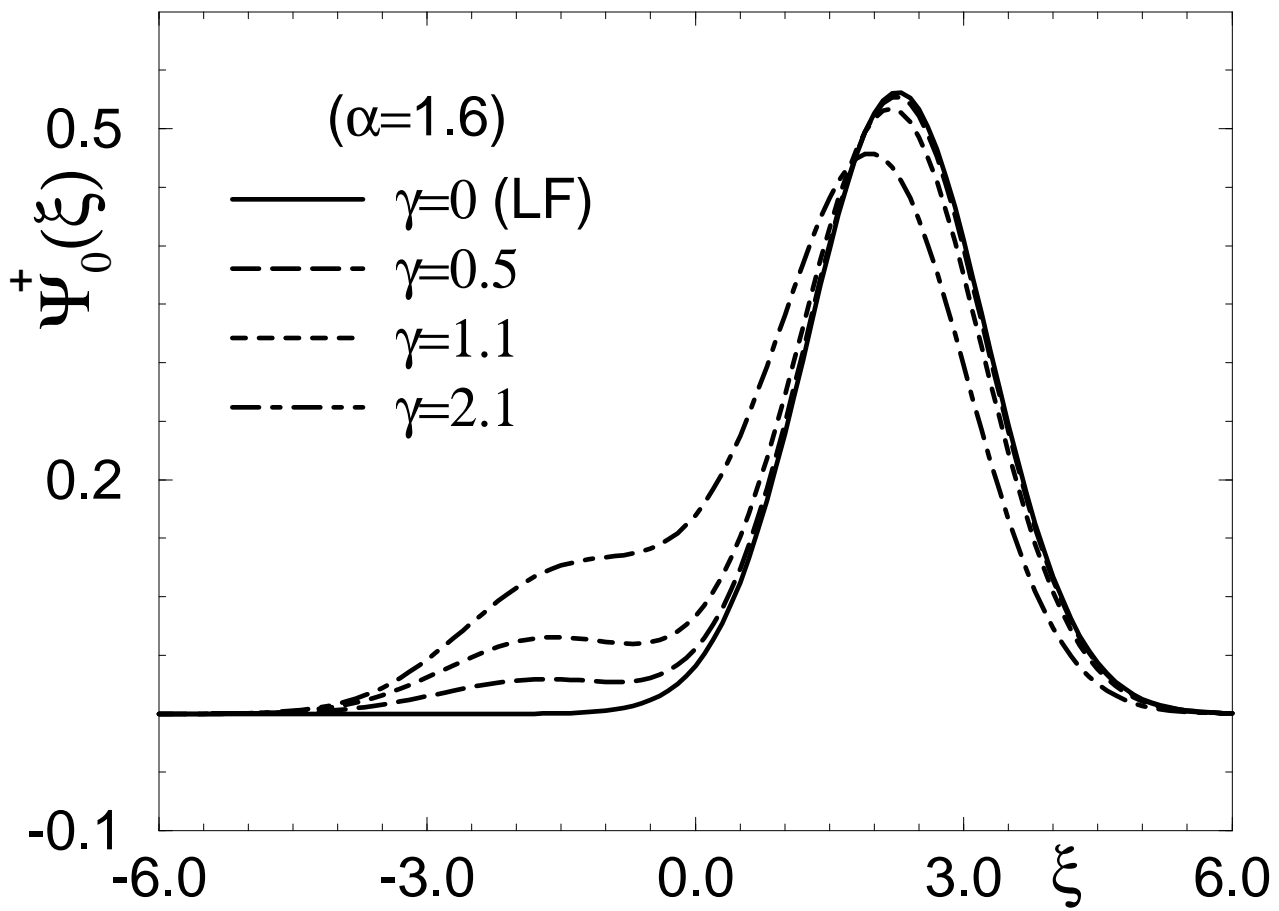


Fig.2

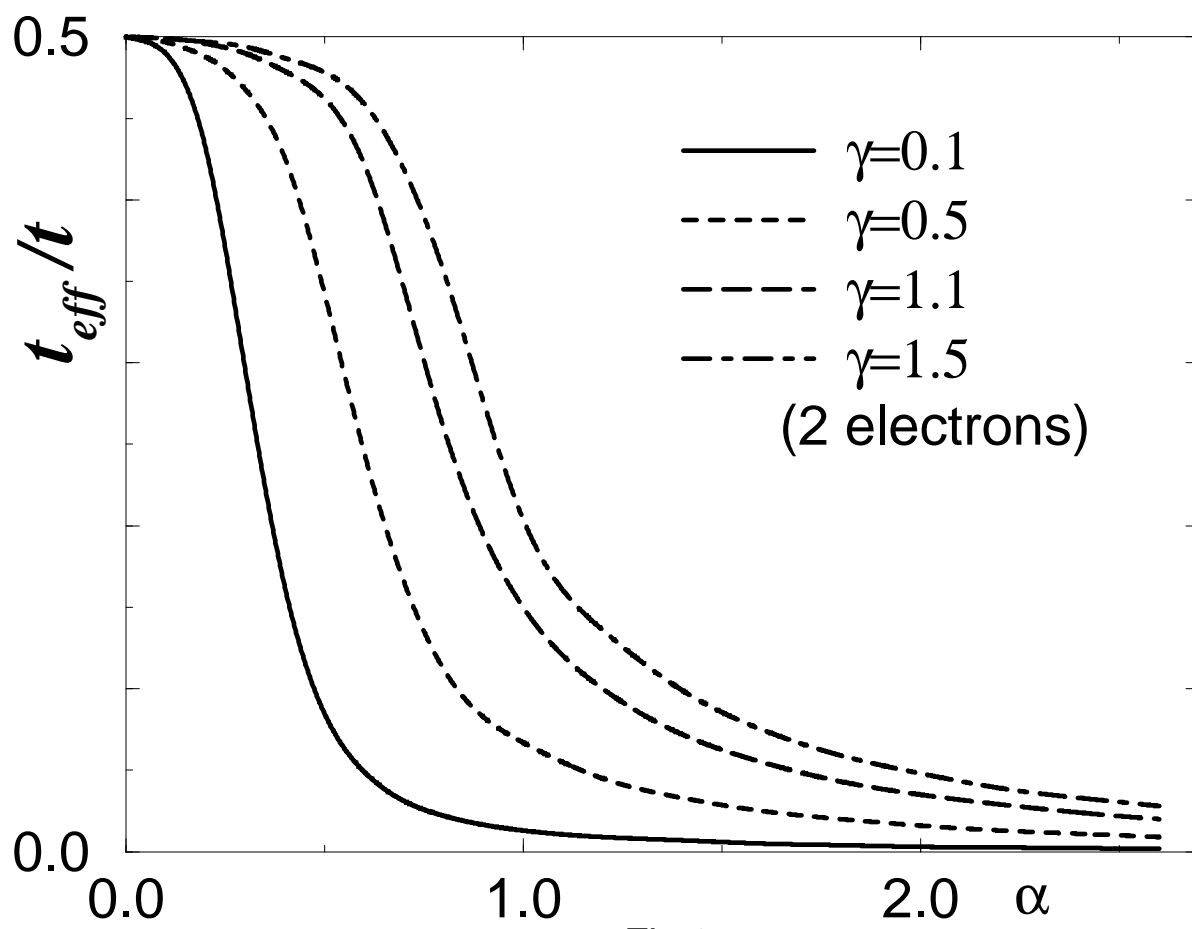


Fig.3a

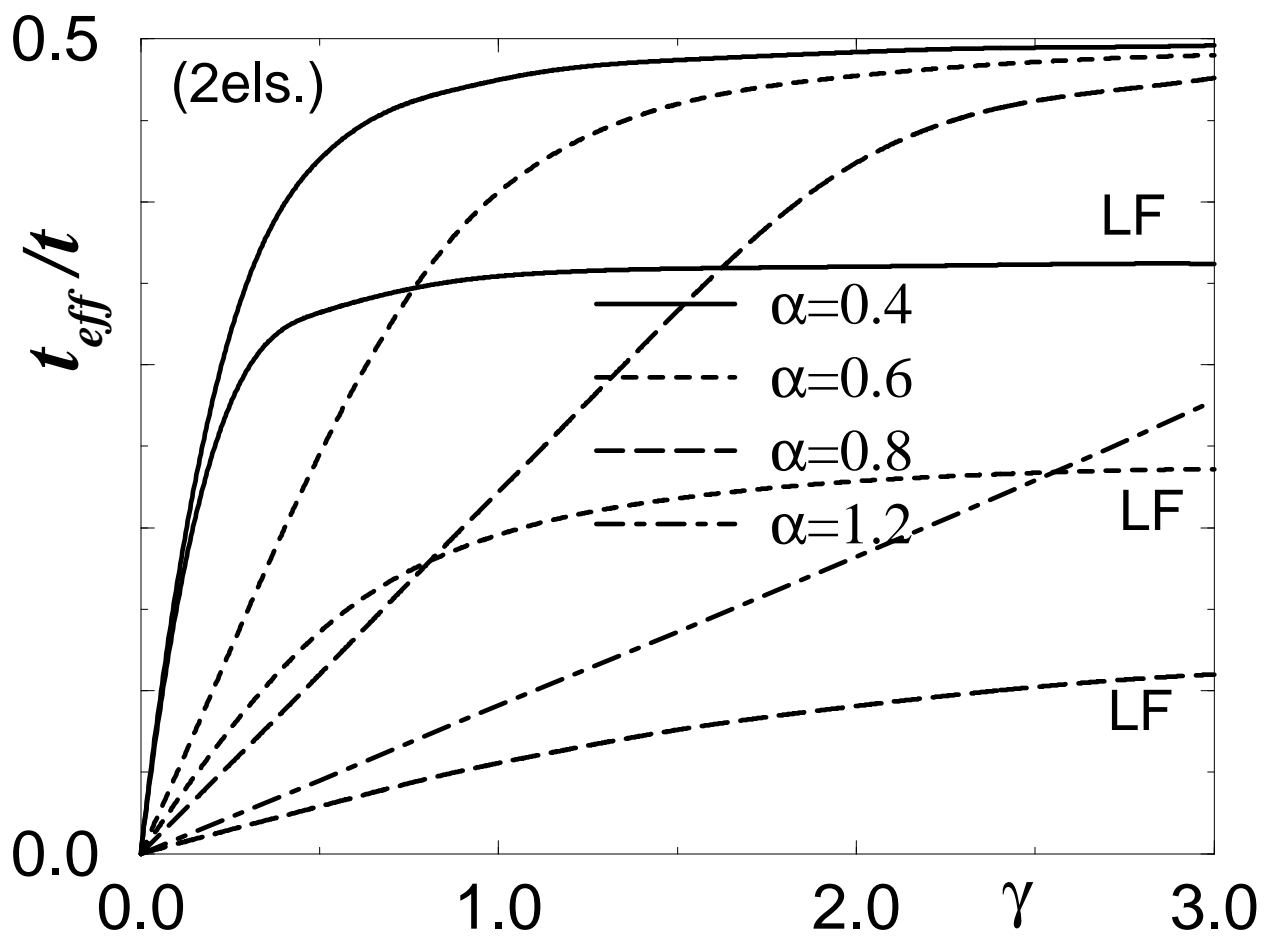


Fig.3b

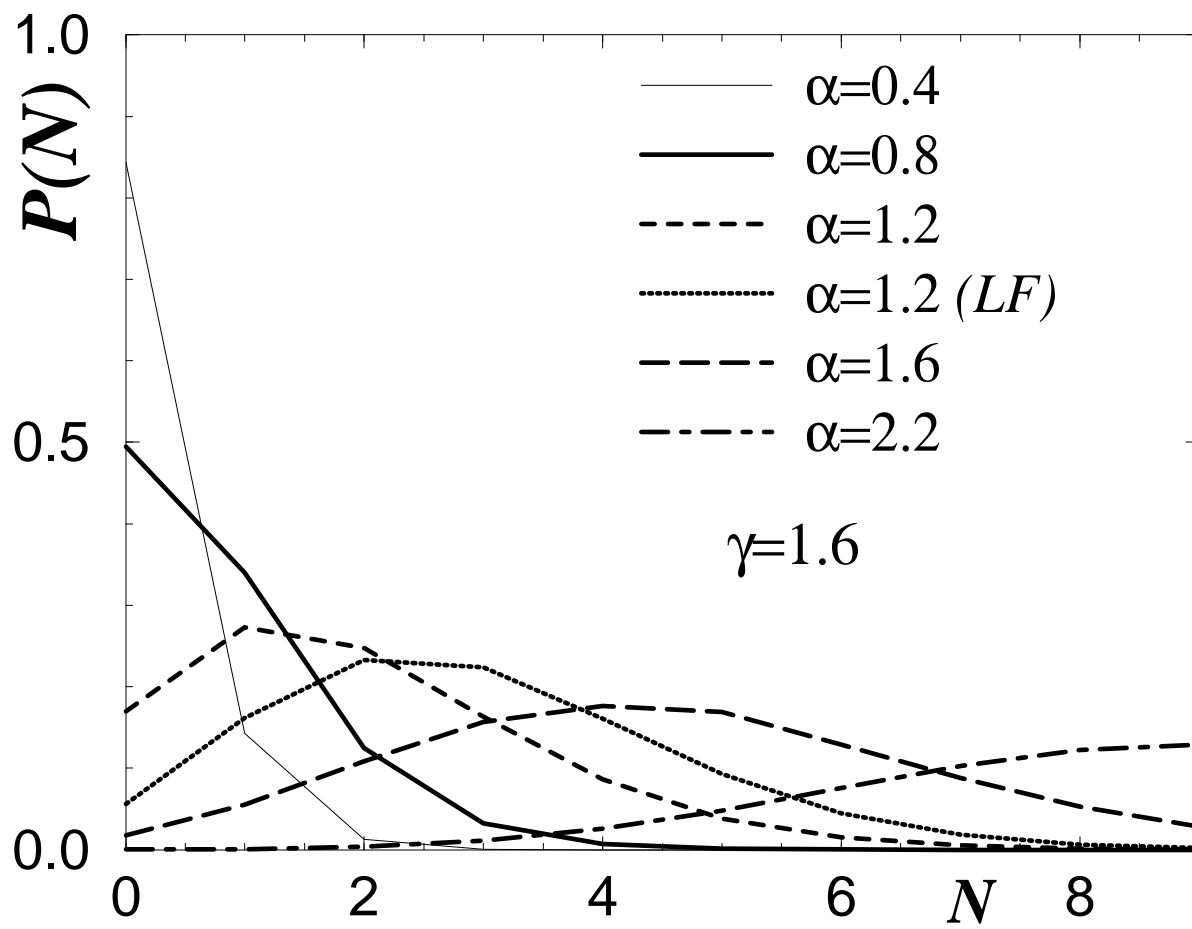


Fig.4a

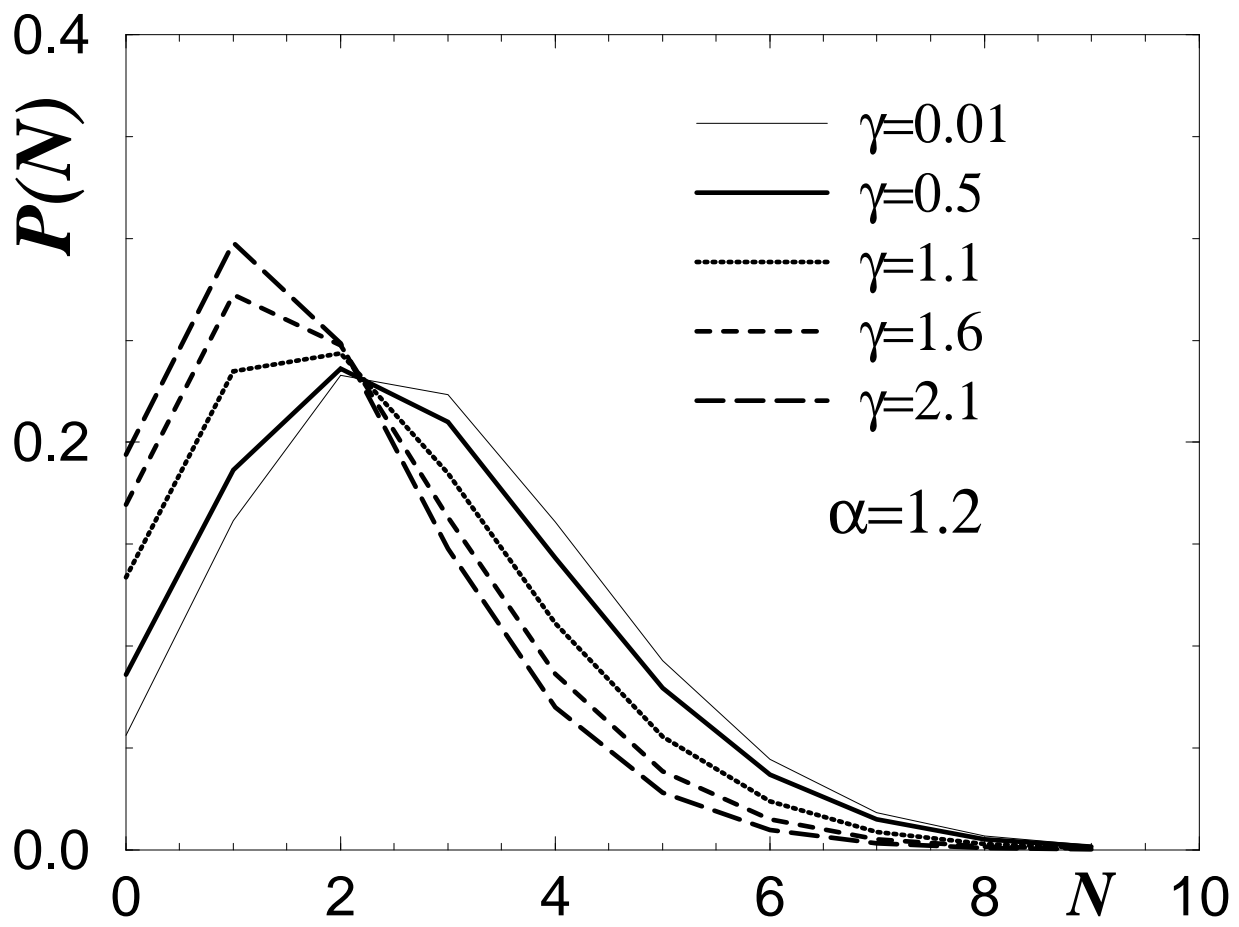


Fig.4b

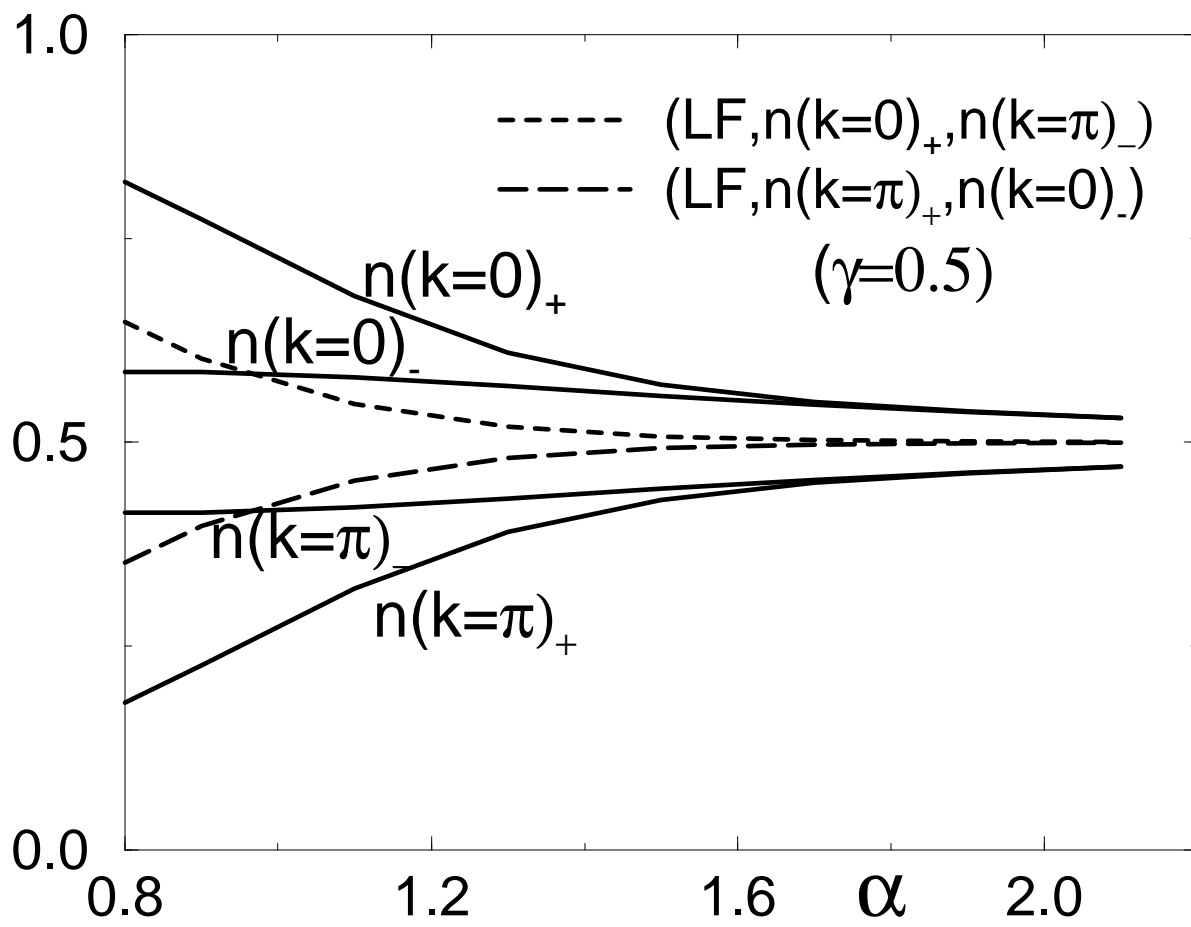


Fig.5

n

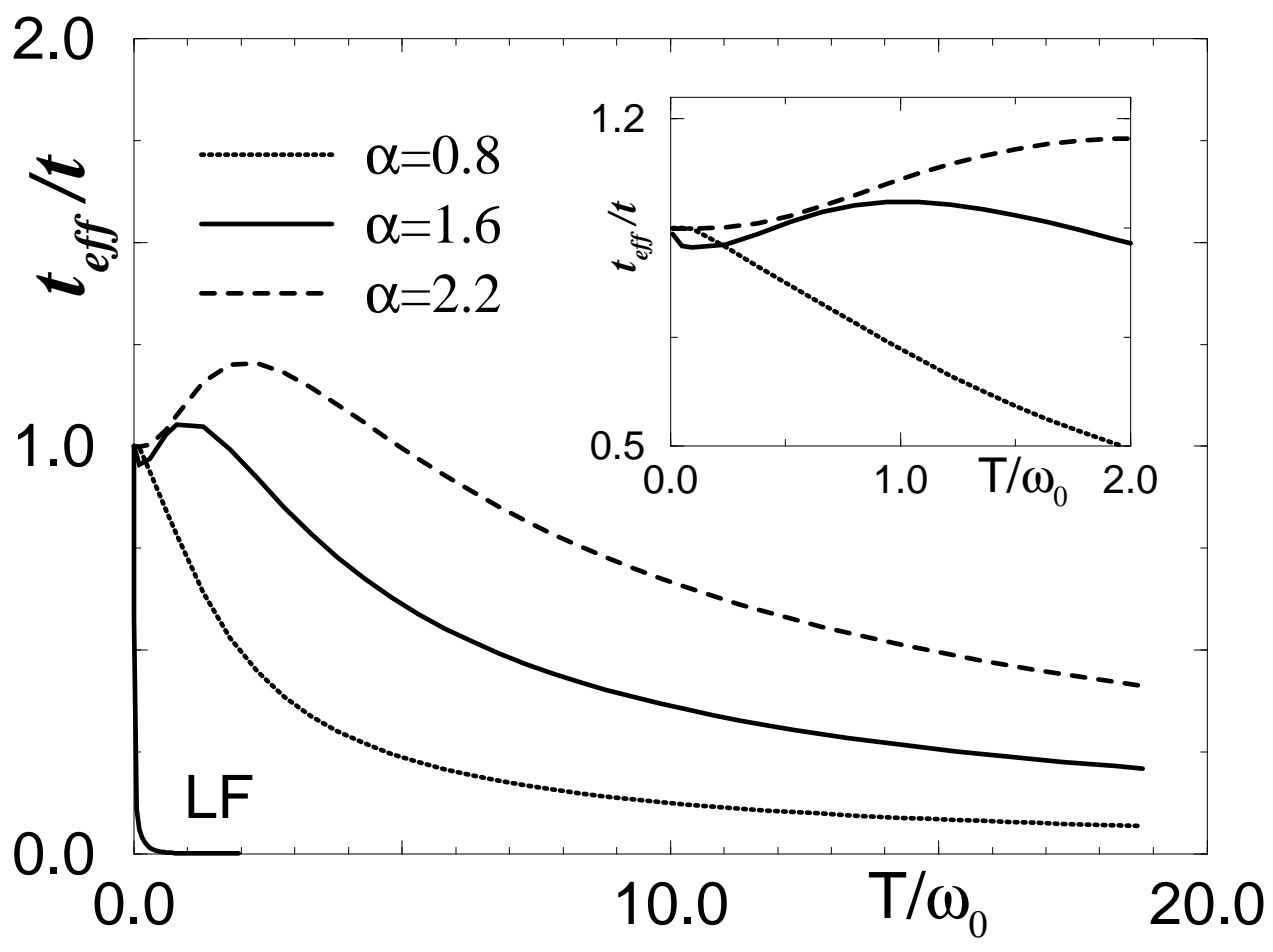


Fig.6

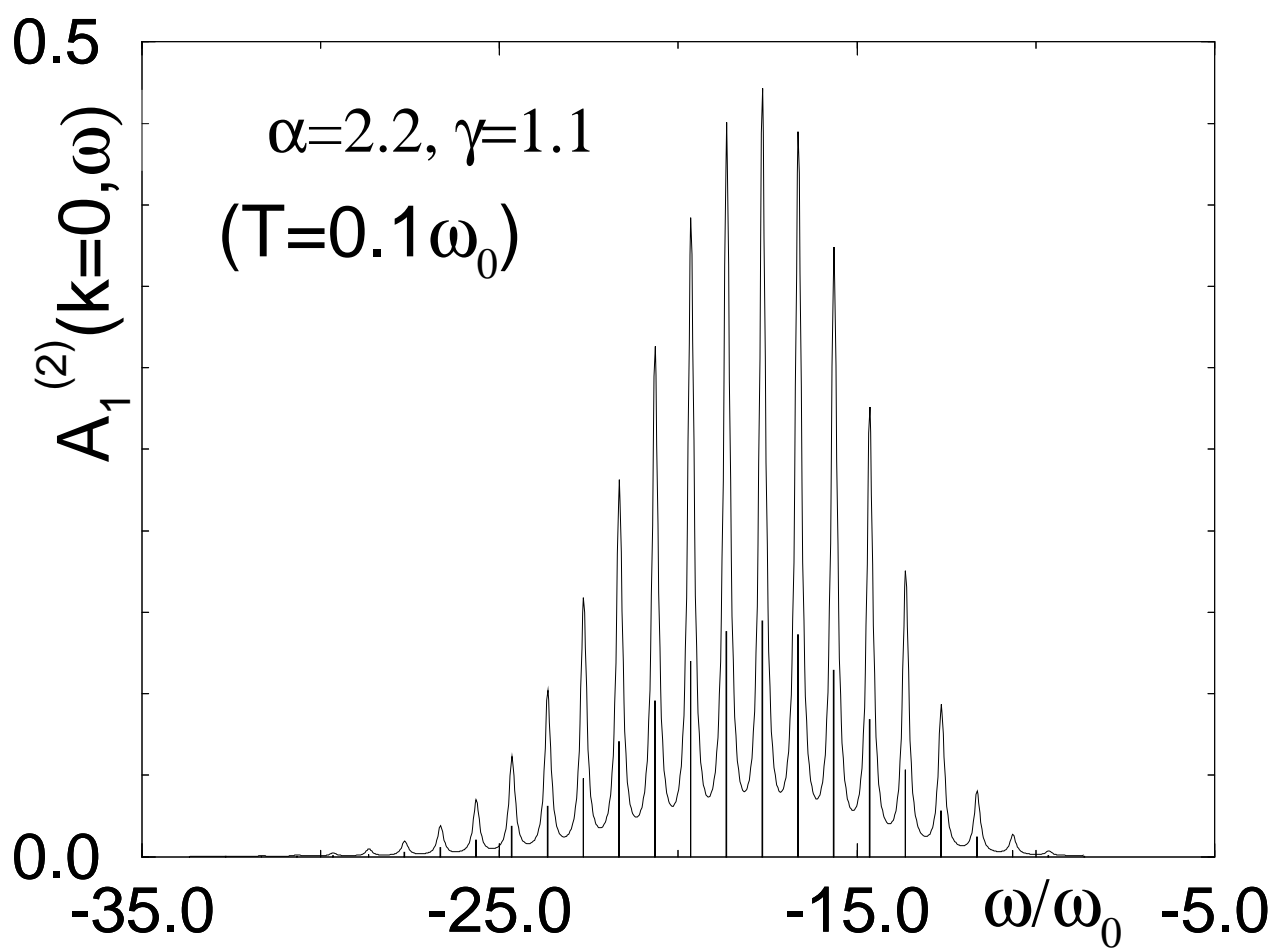


Fig.7a

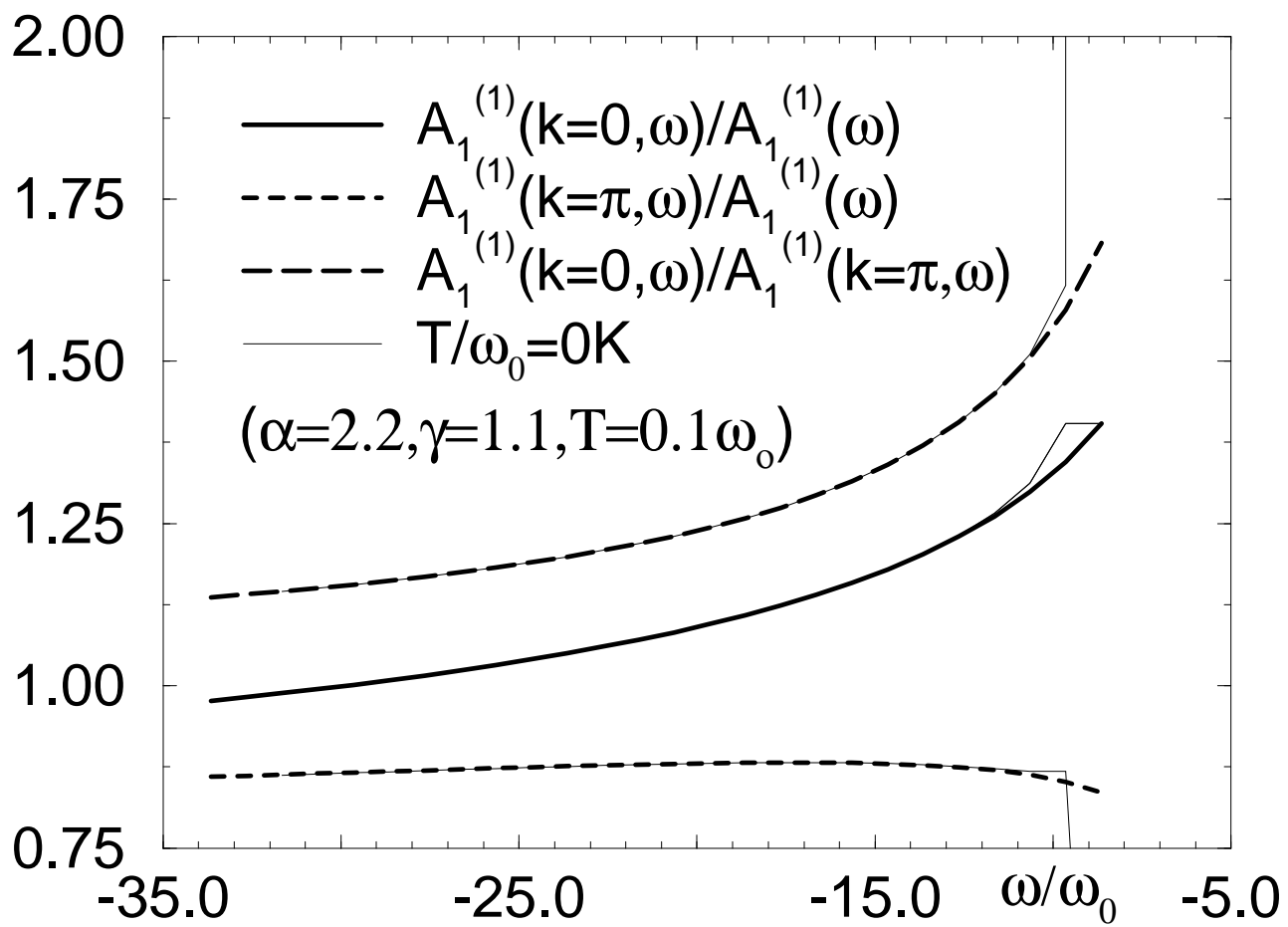


Fig.7b

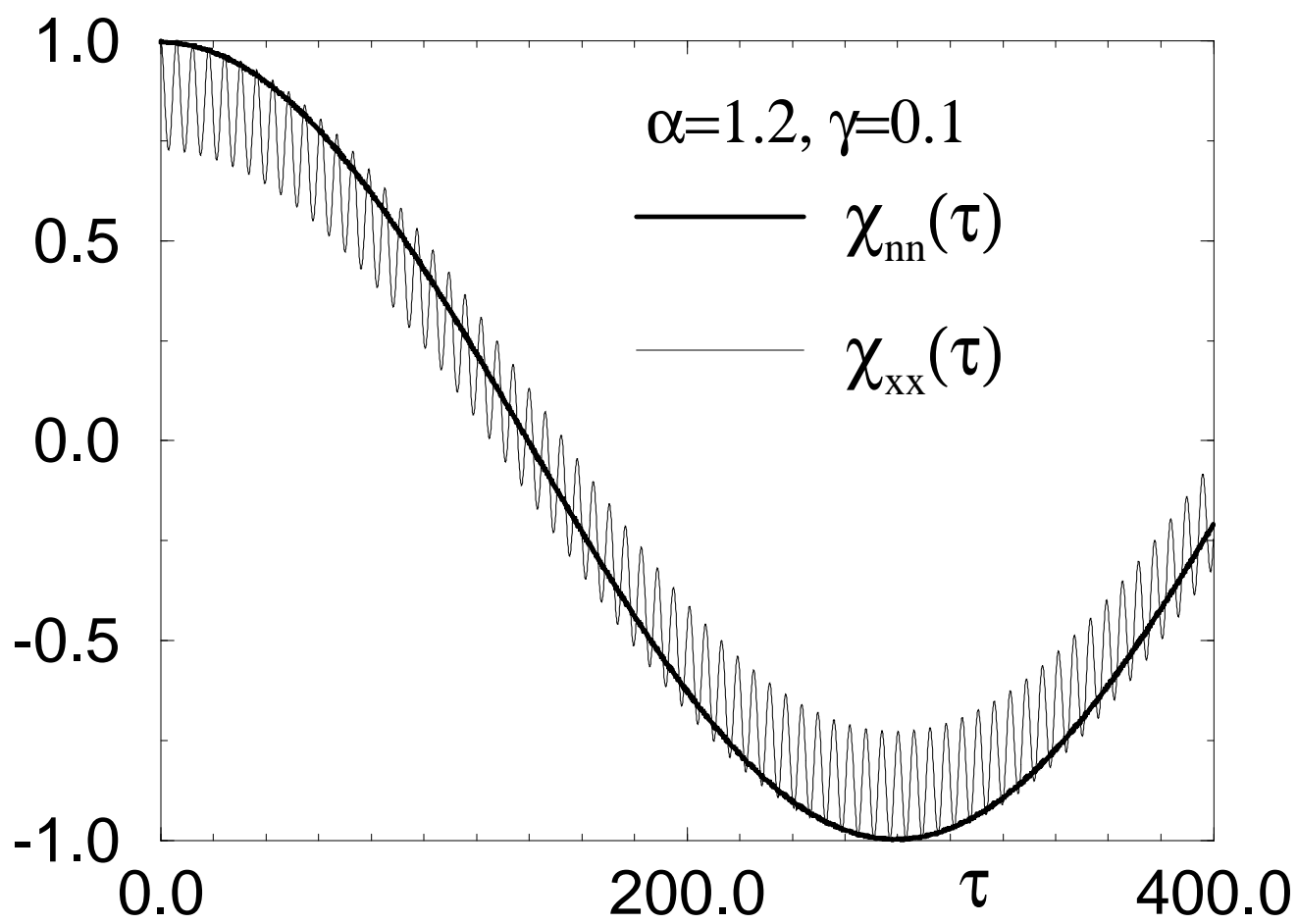


Fig. 12a

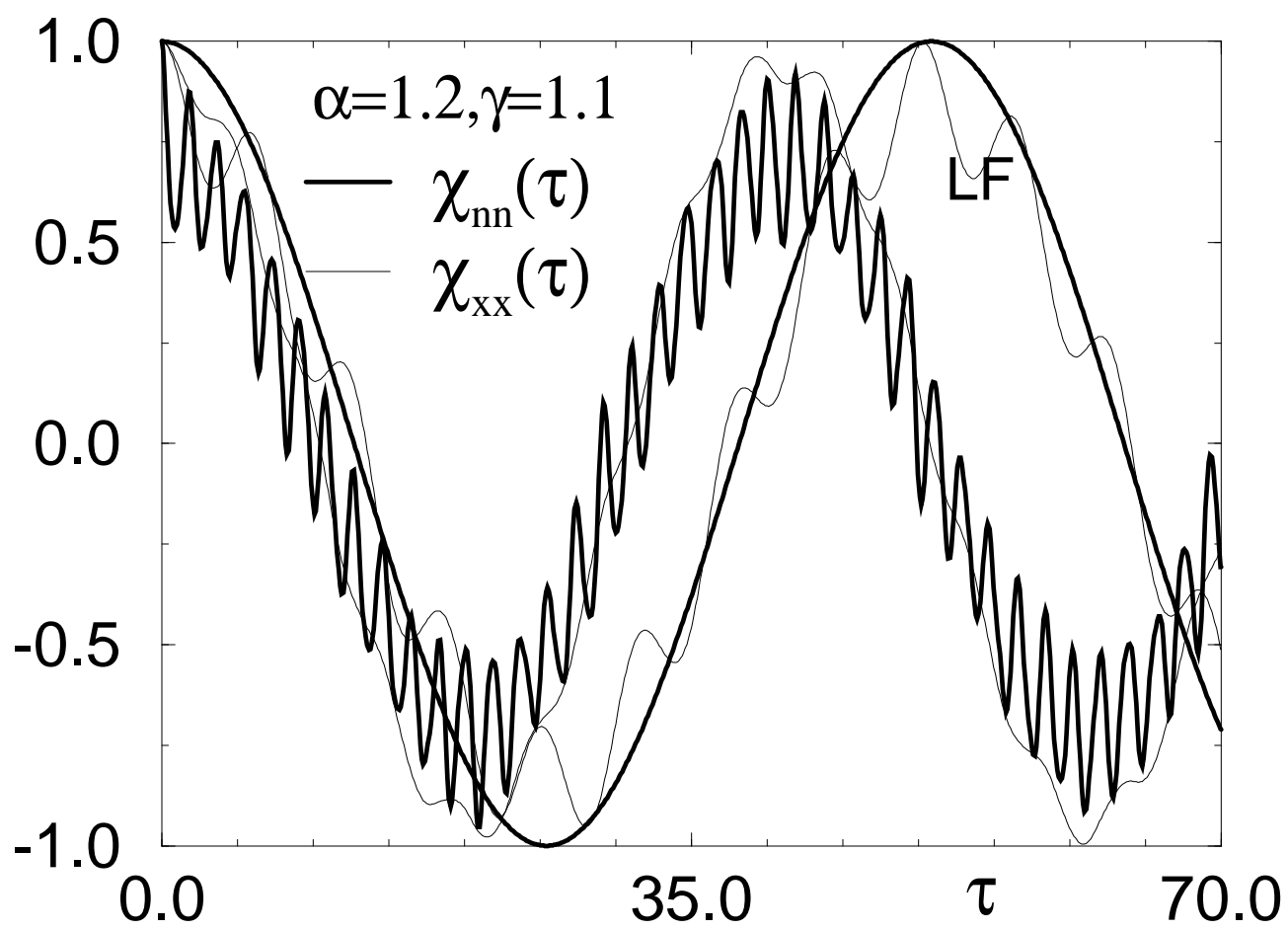


Fig. 12b

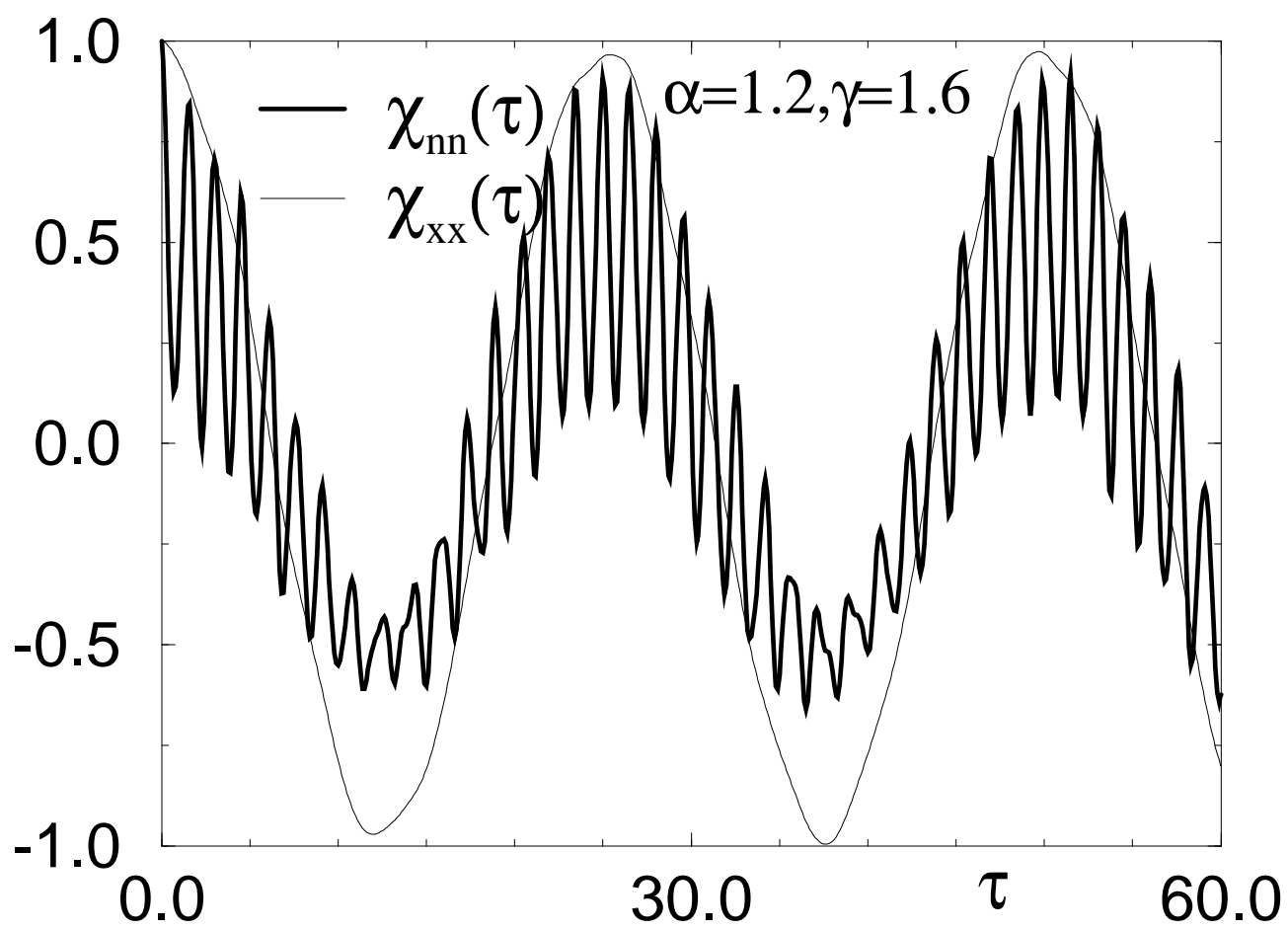


Fig. 12c

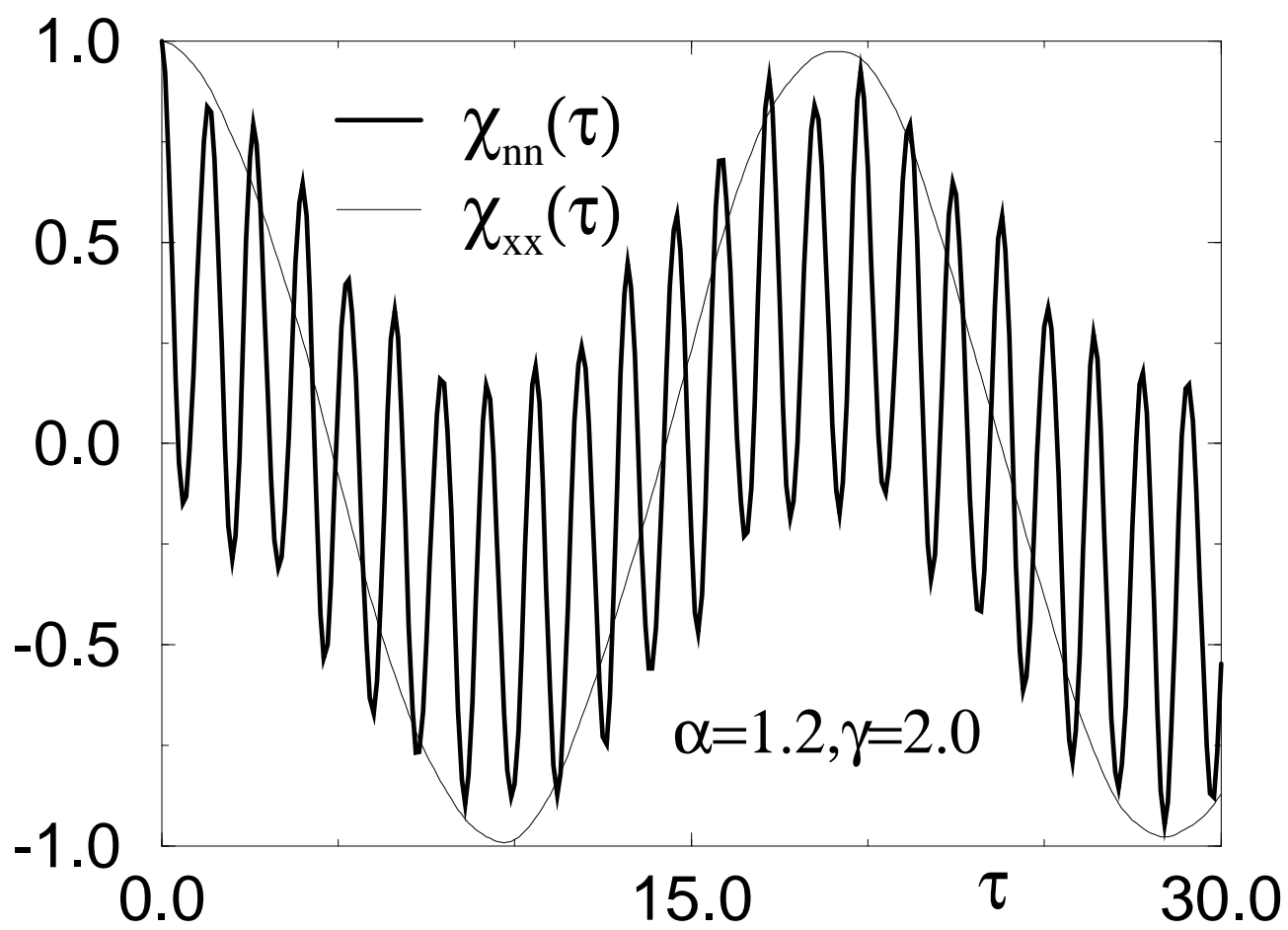


Fig. 12d

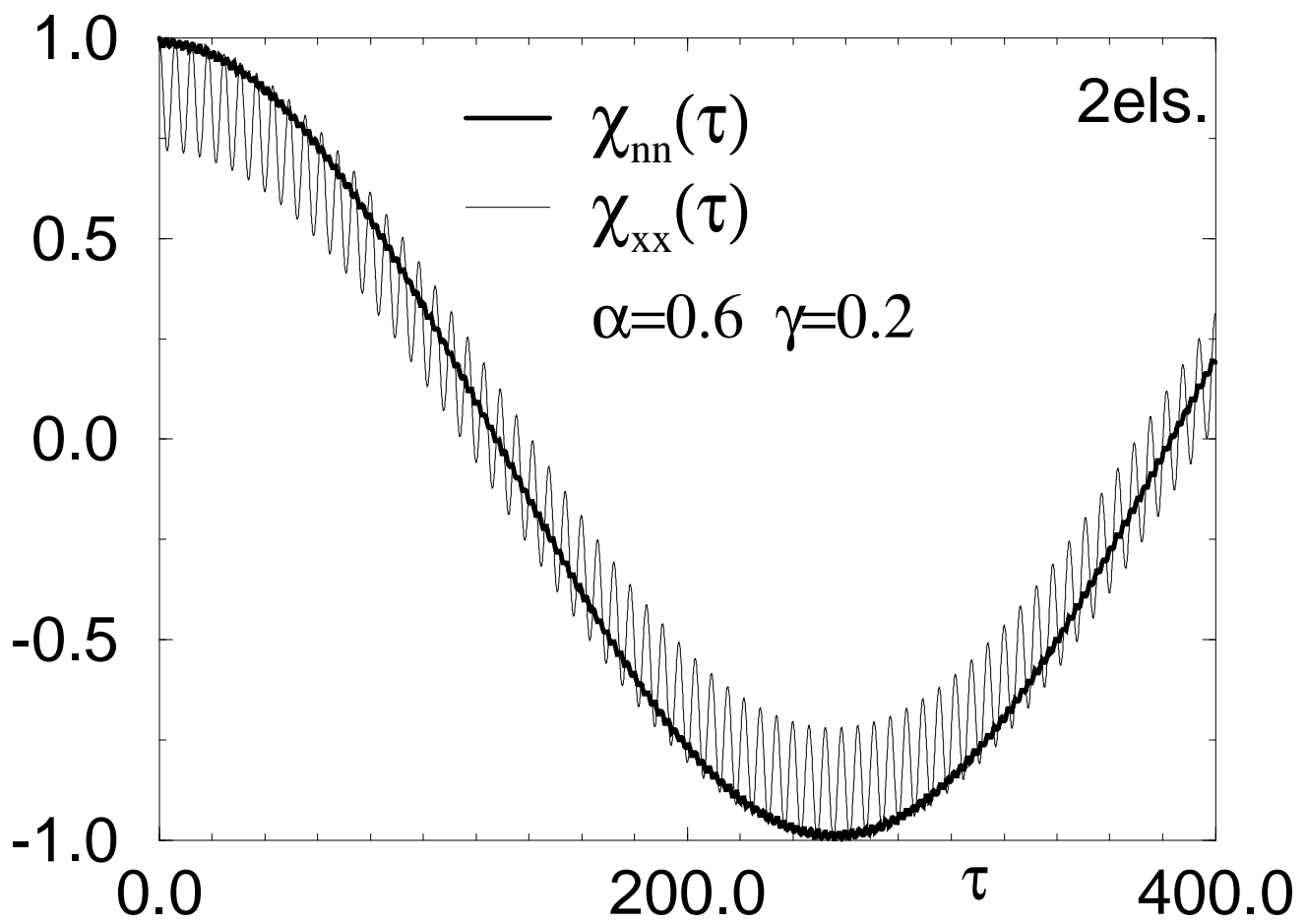


Fig. 13a

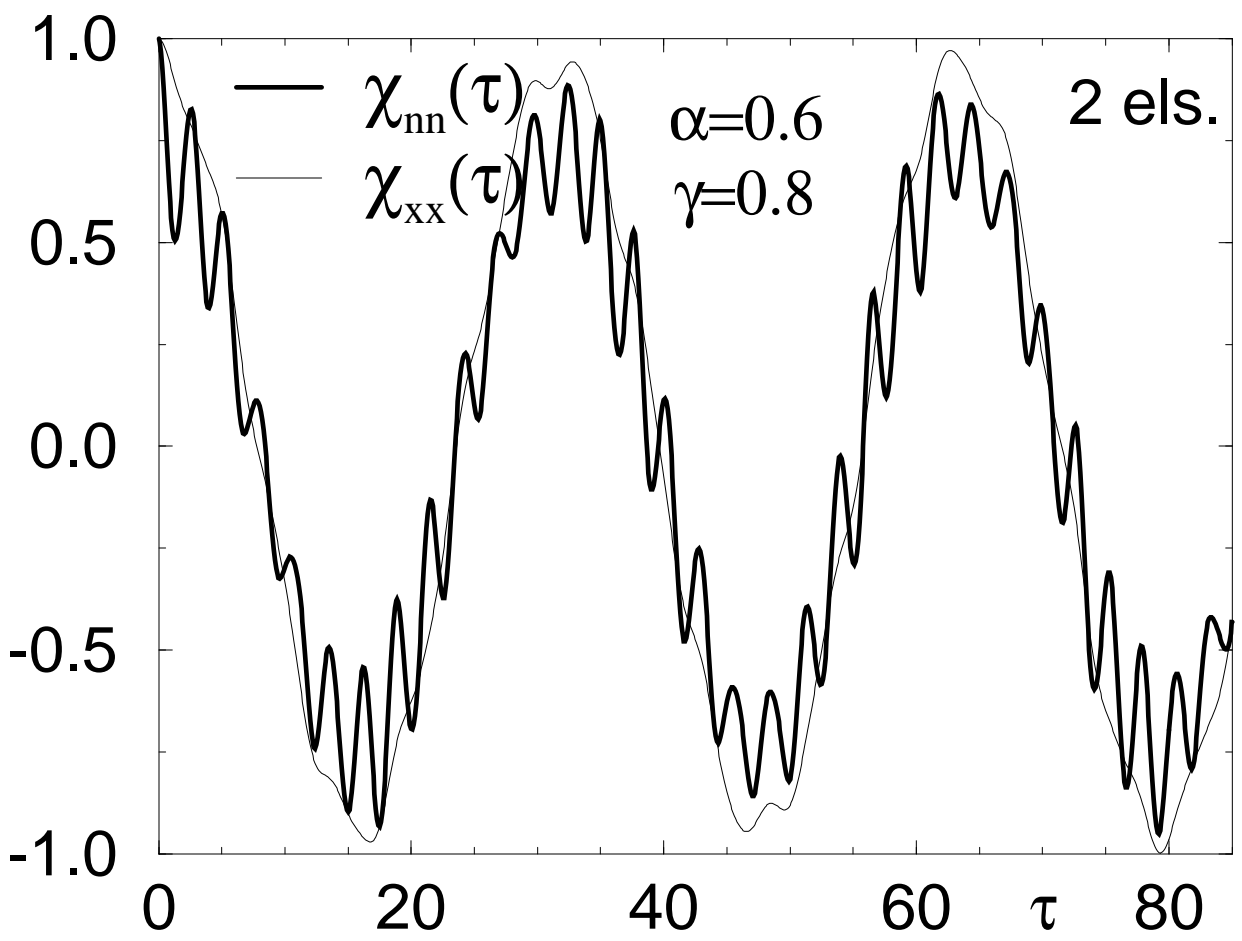


Fig. 13b

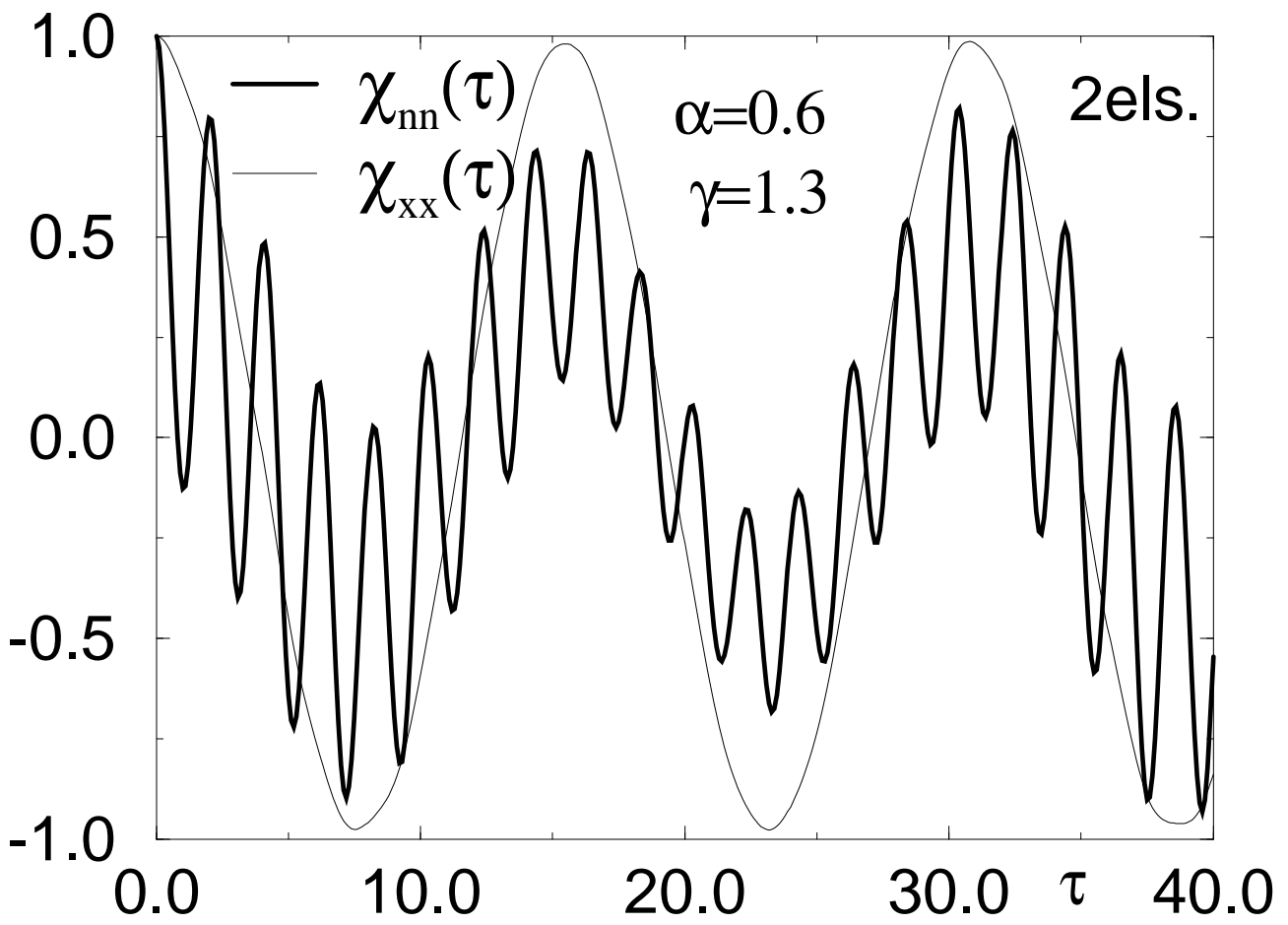


Fig. 13c

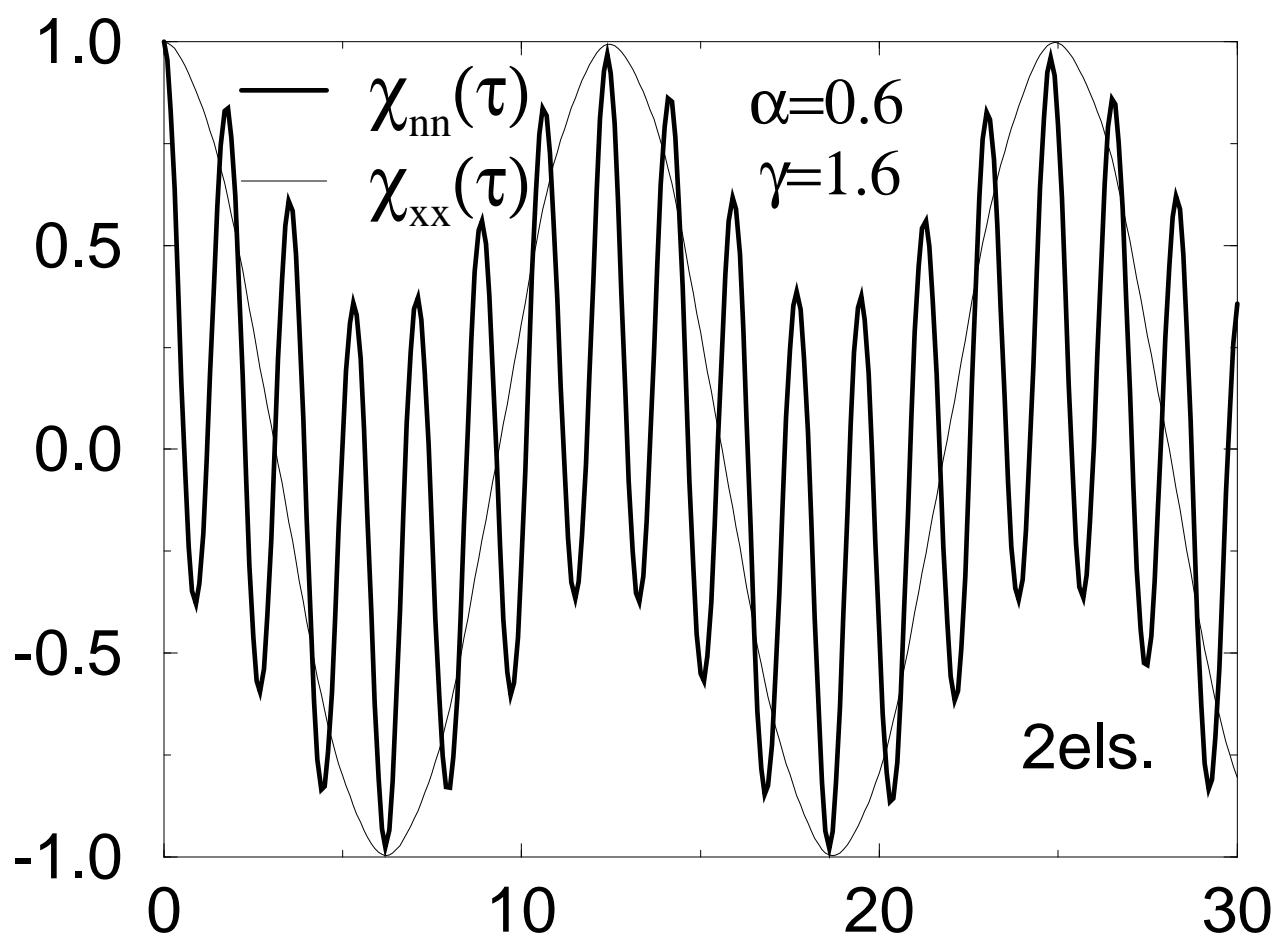


Fig. 13d

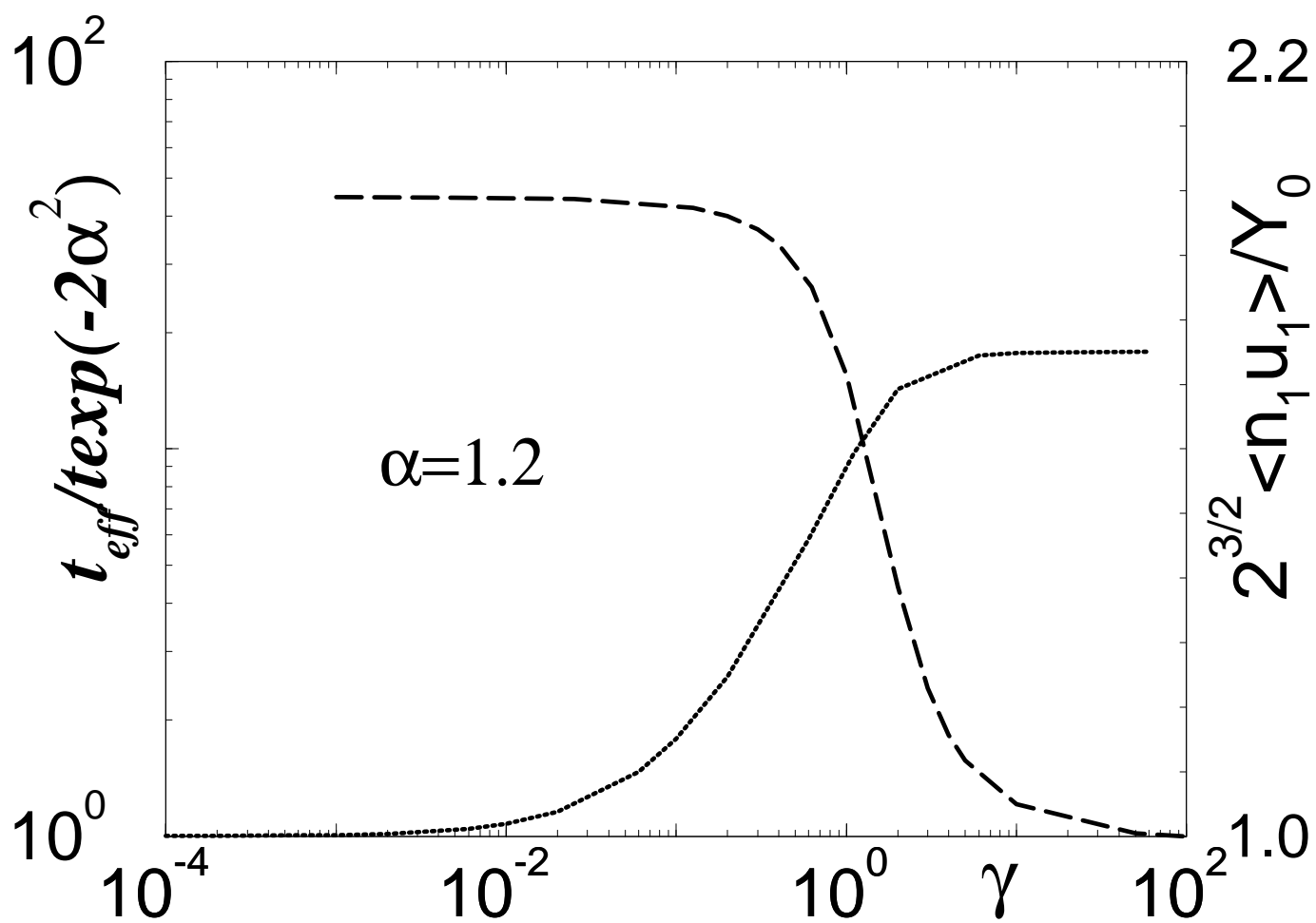
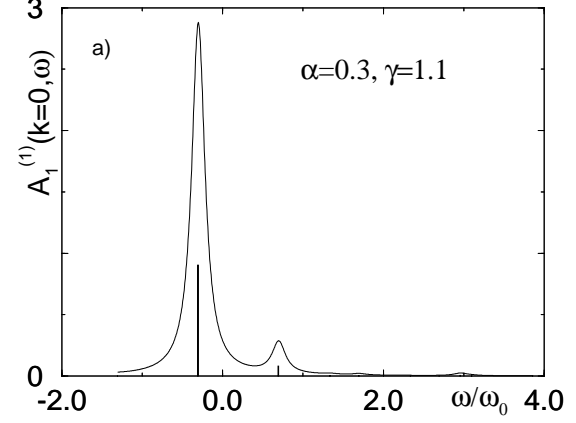
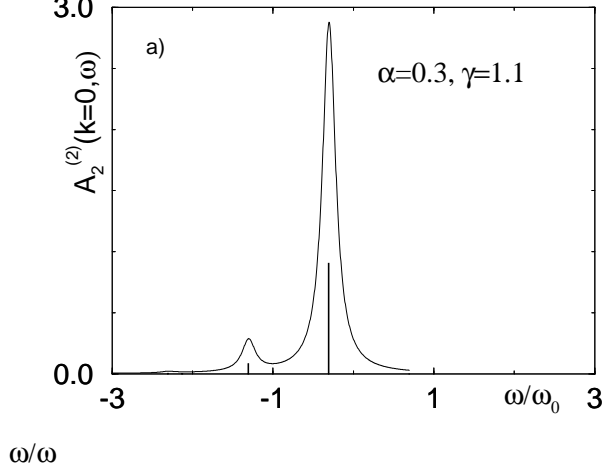


Fig. 14



ω/ω

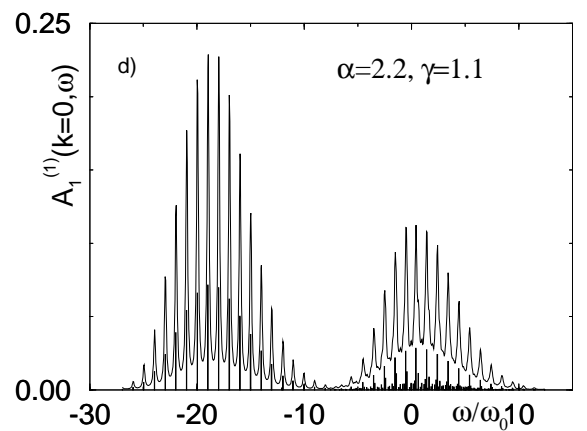
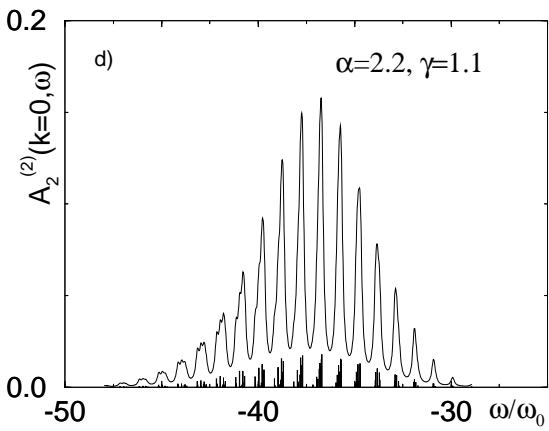
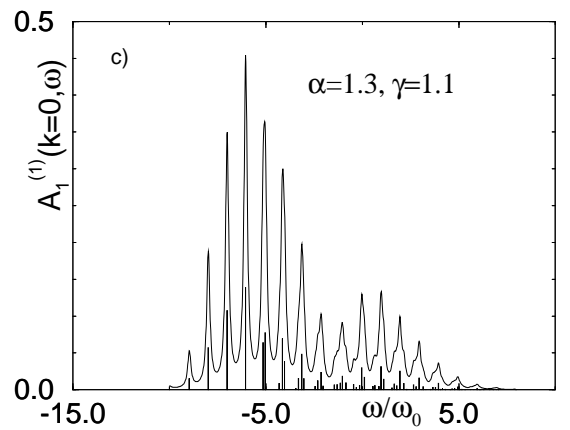
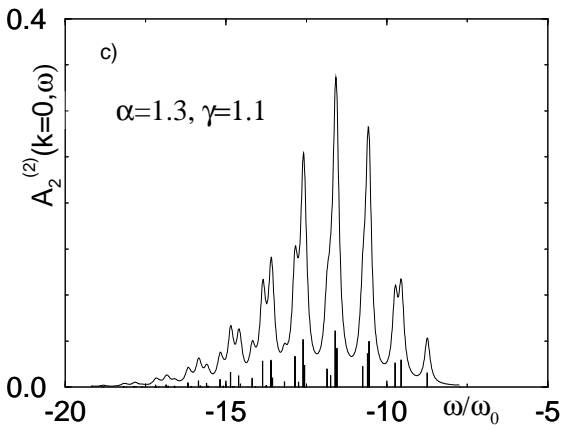
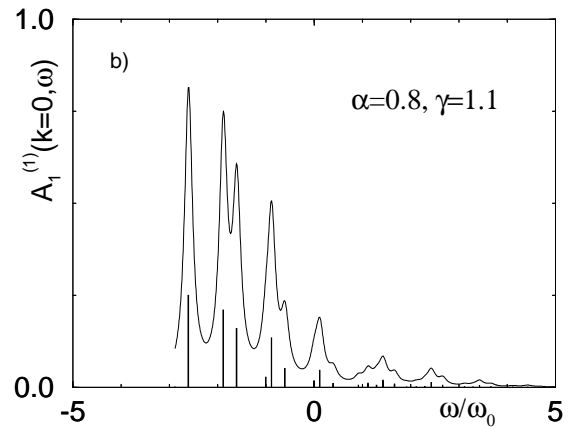
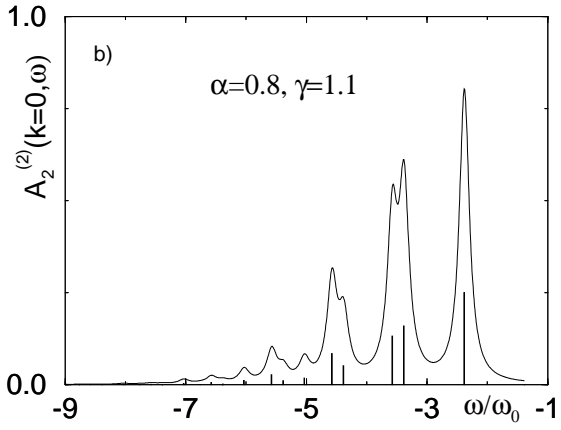


Fig.8a-d

Fig.9a-d

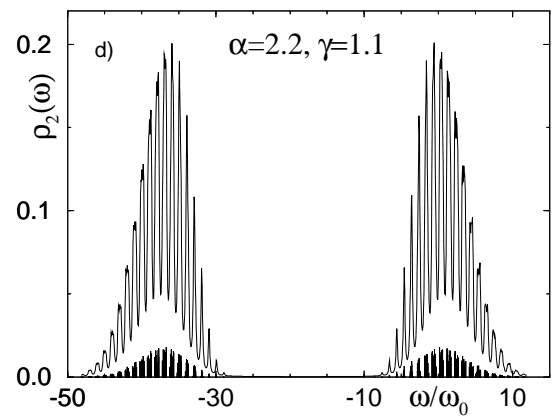
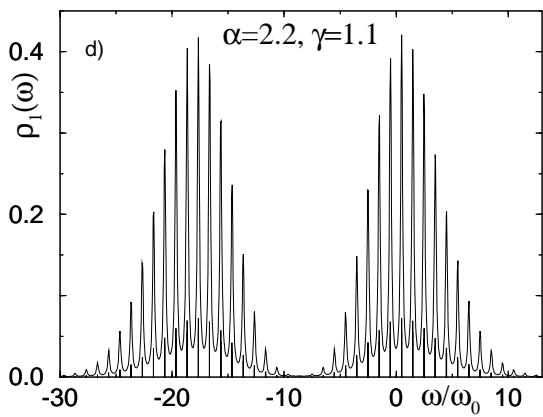
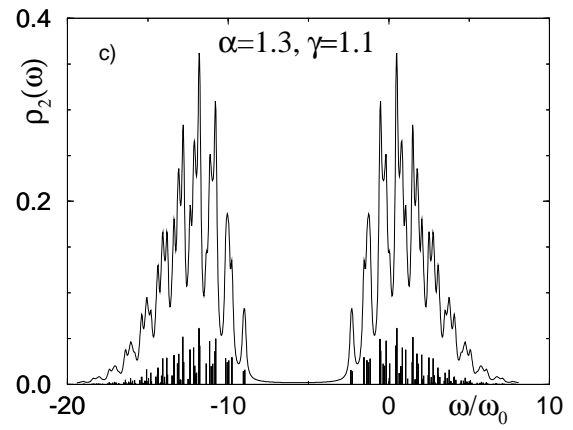
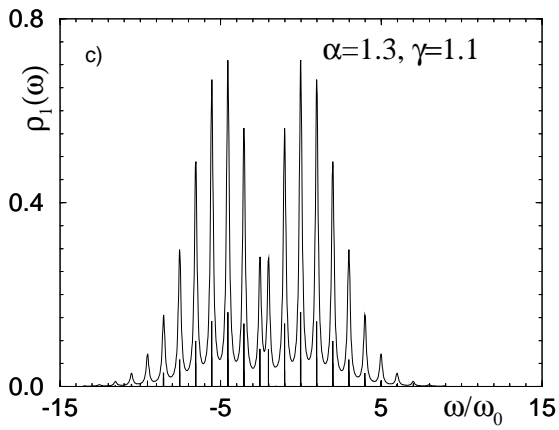
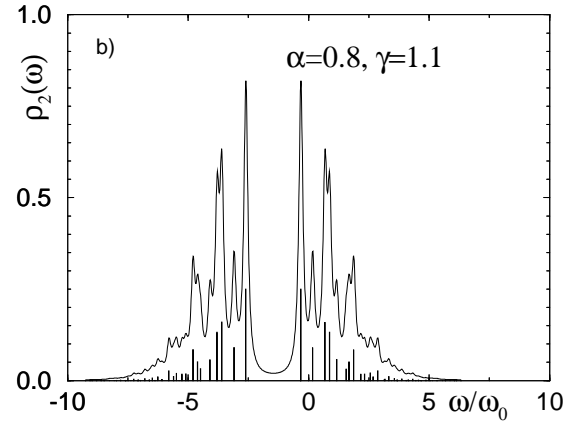
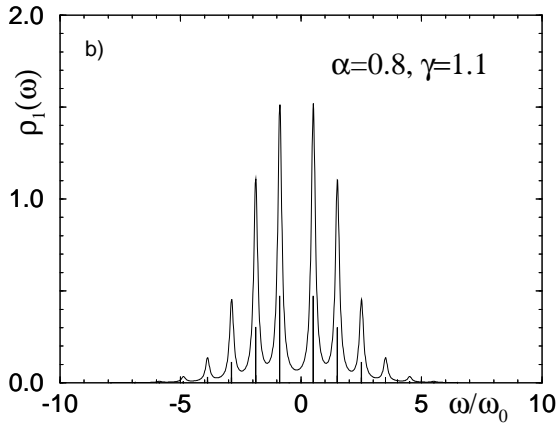
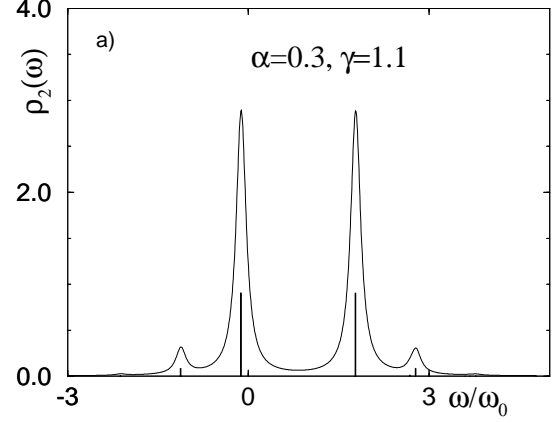
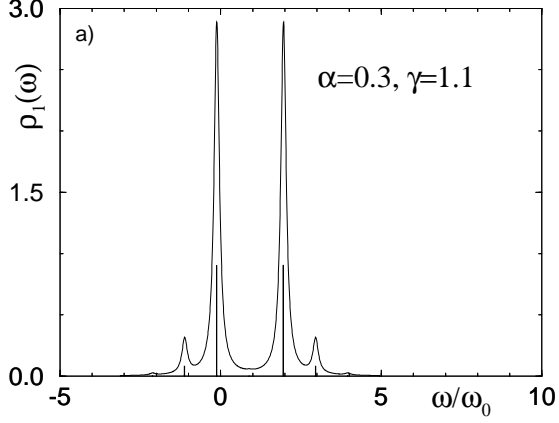


Fig. 10a-d

Fig. 11a-d